International Journal of Nanomedicine

Dovepress
open access to scientific and medical research

Open Access Full Text Article

REVIEW

Inorganic Polyphosphate: Coacervate Formation and Functional Significance in Nanomedical Applications

Heinz C Schröder[1], Meik Neufurth[1], Huan Zhou[2], Shunfeng Wang[1], Xiaohong Wang[1], Werner E G Müller[1]

[1]ERC Advanced Investigator Group, Institute for Physiological Chemistry, University Medical Center of the Johannes Gutenberg University, Mainz, Germany; [2]School of Health Sciences and Biomedical Engineering, Heibei University of Technology, Tianjin, People's Republic of China

Correspondence: Heinz C Schröder; Werner E G Müller, ERC Advanced Investigator Group, Institute for Physiological Chemistry, University Medical Center of the Johannes Gutenberg University, Duesbergweg 6, Mainz, 55128, Germany, Tel +49 6131 392 5791; +49 6131 392 5910, Email hschroed@uni-mainz.de; wmueller@uni-mainz.de

Abstract: Inorganic polyphosphates (polyP) are long-chain polymers of orthophosphate residues, which, depending on the external conditions, can be present both physiologically and synthetically in either soluble, nanoparticulate or coacervate form. In recent years, these polymers have received increasing attention due to their unprecedented ability to exhibit both morphogenetic and metabolic energy delivering properties. There are no other physiological molecules that contain as many metabolically utilizable, high-energy bonds as polyP, making these polymers of particular medical interest as components of advanced hydrogel scaffold materials for potential applications in ATP-dependent tissue regeneration and repair. However, these polymers show physiological activity only in soluble form and in the coacervate phase, but not as stable metal-polyP nanoparticles. Therefore, understanding the mechanisms of formation of polyP coacervates and nanoparticles as well as their transformations is important for the design of novel materials for tissue implants, wound healing, and drug delivery and is discussed here.

Keywords: polyphosphate nanoparticles, phase separation, biomaterial, metabolic energy, morphogenetic activity, tissue regeneration

Highlights

- Polyphosphates are physiological inorganic polymers composed of orthophosphate residues linked via high-energy phosphoanhydride bonds.
- These polymers are unique in their ability to exhibit both morphogenetic and metabolic energy delivering activity.
- The polyanionic polyphosphate is able to form a coacervate in the presence of simple counterions such as calcium ions.
- The polyphosphate coacervate is the biologically active form of the polymer.
- Polyphosphate coacervation can be divided into distinct phases driven by enthalpy and entropy changes.
- Polyphosphate can also be prepared in an inactive nanoparticulate form (storage form).
- Polyphosphate-containing hydrogels are promising materials for bone and cartilage tissue engineering/repair, wound healing, and drug delivery.
- The transformation of polyphosphate nanoparticles integrated in these hydrogels into the biologically active coacervate can be triggered by pH changes or protein contact.

Introduction

In recent years, a group of polymers has attracted increasing attention due to their unique ability to provide metabolic energy needed for tissue regeneration and repair in addition to morphogenetic activity. These polymers, inorganic polyphosphate (polyP), are polyelectrolytes composed of multiple phosphate (P_i) residues linked by

Received: 14 September 2022
Accepted: 3 November 2022
Published: 30 November 2022

high-energy phosphoanhydride bonds[1–3] (Figure 1A). Structurally, the polyP chains are composed of tetrahedrally coordinated P_i units that are interconnected to one another via shared oxygen atoms (Figure 1B).[4]

Coacervate formation with metal ions is a characteristic property of polyP molecules, which is crucial for their biological function and their application as a biomaterial in regenerative medicine and tissue engineering. Only as a coacervate does polyP show morphogenetic activity and can serve as a donor of metabolic energy, but not as nano- or microparticles of the metal salts of the polymer.[3,5]

In general, two types of coacervates can be distinguished: simple coacervates formed between identical macromolecules and complex coacervates formed between different types of macromolecules such as between polyanionic and polycationic polymers (Figure 1C and D).[6] While the formation of the first type of coacervates is primarily associated with a reduction in the interactions of the polymer with the solvent, the formation of the second type of coacervates is based on the association of differently charged macromolecules.

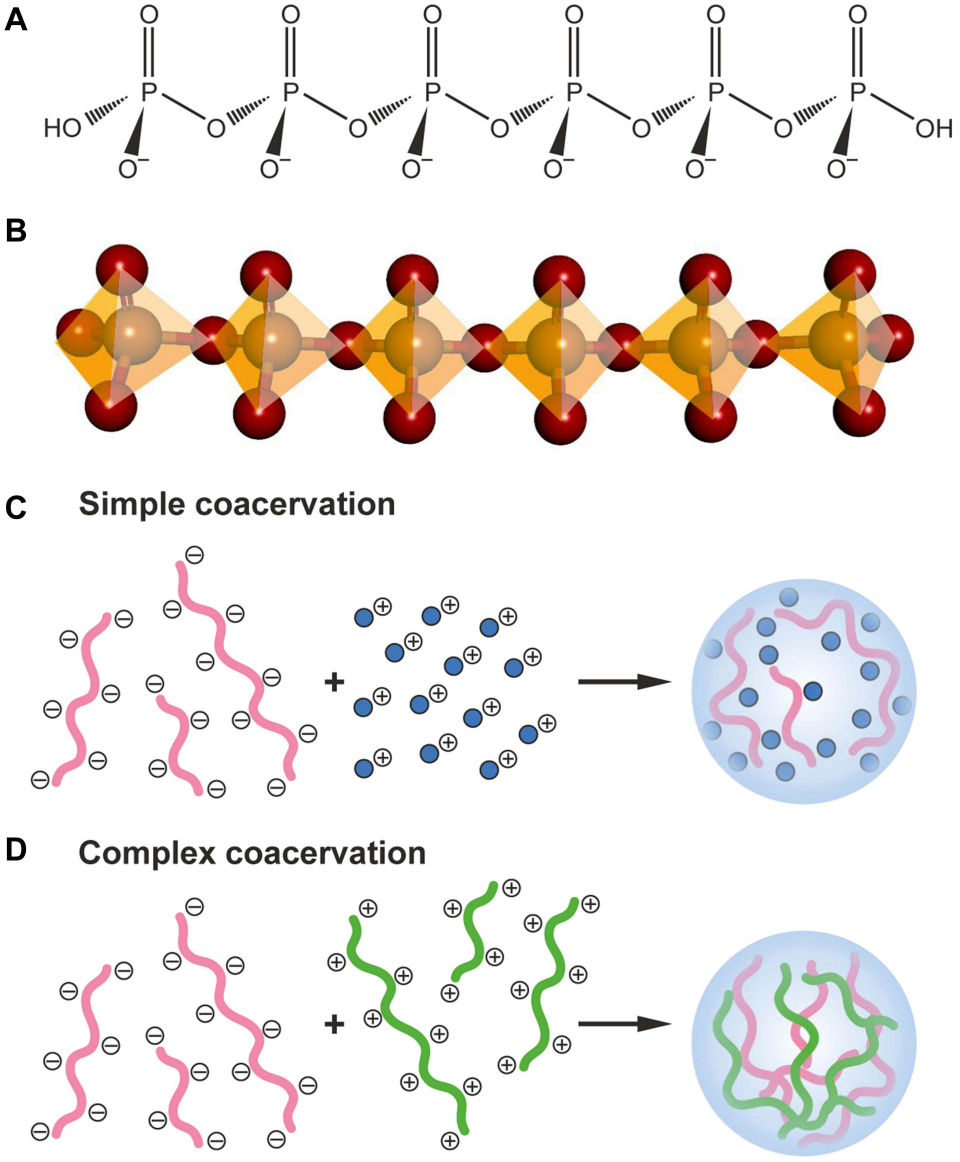

Figure 1 Inorganic polyphosphate (polyP) and types of coacervate formation. (**A**) Structural formula of the polyanionic linear polymer. (**B**) Ball-and-stick model of polyP. The PO_4 tetrahedra are linked via their shared oxygen atoms giving the molecule rotational flexibility. (**C**) Simple coacervation between identical macromolecules. (**D**) Complex coacervation between different types of macromolecules such as polyanionic and polycationic polymers.

The formation of coacervates is based on liquid–liquid phase separation of an initially homogeneous aqueous solution of macromolecules into two liquid phases, a more concentrated phase, the coacervate, and a diluted phase.[7,8] A variety of macromolecules are capable of coacervate formation, including both natural molecules such as nucleic acids, polysaccharides and proteins[9–11] and synthetic polymers, particularly combinations from oppositely charged polyelectrolytes.[7,12] The formation of coacervates has been implicated in an increasing number of biological processes,[8] including processes involved in protein aggregation.[13]

In this review, we summarize the current state-of-the-art on coacervate formation from polyP, in particular the formation of simple coacervates of the polymer, the underlying mechanism, and potential applications and biological effects of the polyP coacervates as a component of novel implant materials, gels and drug delivery systems.

Coacervates

Physiologically, coacervates are found both intracellularly and extracellularly. Examples of intracellular coacervates are membraneless organelles such as stress granules, nucleoli or Cajal bodies, which are formed by the assembly of small nuclear ribonucleoprotein particles.[6,8,14–16] Compartmentalization via the formation of cell-like coacervate droplets has also been implicated in the origin of life,[17] and there is increasing interest in peptide-based coacervates as primitive protocell models.[18,19] Due to their special properties, coacervate materials that mimic natural systems have opened new applications in biomedicine and technology.[20] For example, polyelectrolyte-based coacervates secreted by sandcastle worms[21] have been used as a model for the development of biomimetic underwater adhesives.[22,23]

Compared to complex coacervates, which are composed of two or more types of polyelectrolytes with opposite charges, natural or synthetic, there have been relatively few studies on simple coacervates, which consist of only one type of macromolecule, with the exception of simple coacervates or condensates formed by proteins containing intrinsically disordered regions.[24,25] The formation of simple coacervates is characterized by hydrophobic interactions, in contrast to complex coacervation, which is driven by the initial electrostatic attraction between oppositely charged polyelectrolytes and entropy due to the release of bound counterions and the reorganization of the surrounding water molecules.[9,12,20,26–29] Consequently, in addition to pH, temperature and the concentrations and concentration ratios of the polyelectrolytes, the ionic strength and the charge density of the polyelectrolytes play an important role in complex coacervation.[14,30–33] The coalescence of the initially small polyelectrolyte-rich coacervate droplets subsequently leads to larger droplets that are surrounded by and in equilibrium with a less dense, polyelectrolyte-poor liquid phase.[20]

In protein-based coacervate formation, in addition to the solution pH and ionic strength, the isoelectric point is a critical factor in the ability of the protein to form a coacervate.[26] In addition, π–π interactions of the Arg guanidinium groups together with dipole–dipole, cation–anion, and π–cation interactions contribute to complex coacervation, particularly in proteins with partially intrinsically disordered regions.[13,15] Increasing the ionic strength can suppress coacervate formation by shielding attracting charges on the macromolecules.[26] The strength of the coacervate formed depends on the ratio between the strength of the electrostatic interaction and the thermal energy k_BT.[34]

In complex coacervation, the phase behavior can be described using the Flory−Huggins theory and presented in the form of a phase diagram, giving the boundary between the dilute and dense phases of a polymer mixture.[7,35–38] The width of the two-phase region in the phase diagram depends on different variables such as temperature, pH and salt concentration.[12,35]

Phase separation in simple coacervate formation after addition of alcohol or salt to a homogeneous polyelectrolyte solution has been discussed by Gupta and Bohidar.[39] Electrostatic and solute-solvent interactions are decisive factors that drive phase separation in simple coacervation. The higher entropy of the solution is due to the higher number of possible spatial arrangements of the solvent (water) molecules around the polymers. The coacervation process leads to an increased pressure within the coacervate phase, resulting in water expulsion (syneresis).[40]

Inorganic Polyphosphate

Inorganic polyphosphates (polyP) are strong polyanions at neutral and alkaline pH, carrying a negative charge on each internal P_i unit and between one and two negative charges on the terminal P_i residues (Figure 1A). The dissociation constants for the internal and first terminal OH groups are high ($pK_1 = 2.2$), while the dissociation constant for the second

terminal OH group is lower (pK_2 = 7.2).[41] The linear polymers can be divided in different size classes, short-chain (n < 10), medium-chain (n = 10 − 50), and long-chain polyP (n > 50). In addition, there are cyclic polyP molecules that mainly consist of 3, 4 or 6 P_i units.[42] According to the Q^i nomenclature, based on the number of bridging oxygens, linear polyP consists of both Q^1 (terminal P_i residues) and Q^2 tetrahedra (internal P_i residues) (Figure 1B), while cyclic polyP has only Q^2 structures. Orthophosphate, the product formed by complete hydrolysis of polyP, is classified as Q^0 (no bridging oxygens). The energy barrier for rotation around the P–O–P bonds of the interconnected P_i tetrahedra is low. Therefore, linear polyP molecules are characterized by high flexibility. The bond angles on the phosphorus and oxygen atoms of the polyP chains (102° and 130°, respectively)[43] can vary over a wide range (~120° to 180°) after binding of cations to the polymer.[44]

As the sodium salt (Na-polyP), polyP with chain lengths of less than 100 P_i residues is readily soluble in water.[45,46] However, in the presence of divalent or trivalent cations such as Ca^{2+}, Mg^{2+}, Sr^{2+}, Al^{3+} or Gd^{3+},[47–53] precipitation or phase separation of the polymer occurs depending on the concentration and external conditions, such as pH, temperature and ionic strength, as described later below. Divalent cations are bound to two adjacent phosphate groups, while trivalent cations are complexed with two and three phosphate ligands.[54]

Although polyP is fairly stable in aqueous solutions at room temperature under neutral or alkaline conditions and can be stored over long periods of time,[2,46] this polymer is thermodynamically unstable in water with respect to its monomeric hydrolysis (P_i) products. The standard Gibbs free energy ΔG^0 of hydrolysis of the phosphoanhydride bond in linear polyP is close or equal to that for the hydrolysis of the β-γ or α-β P–O–P bonds in ATP (−30.5 kJ·mol^{-1}). ΔG^0 values of −40.6 kJ·mol^{-1} were even reported.[55] Therefore, the chemical equilibrium of polyP in aqueous solutions under standard conditions is almost entirely on the side of orthophosphate.

The kinetic stability of polyP at room temperature and neutral or alkaline pH can be explained by the high density of negative charges on the polyanionic molecule, which protect the polymer from hydrolytic degradation by attacking water molecules.[46,56–58] Under acidic conditions, polyP is hydrolyzed[45,46,48] starting from the ends of the polymer.[2,59,60] The acid-catalyzed hydrolysis proceeds via the formation of a pentacovalent intermediate formed by nucleophilic attack of a water molecule after protonation of the double-bonded oxygen at the terminal phosphorus atom. This reaction is characterized by a significantly reduced activation energy (E_a = 57 kJ·mol^{-1}) compared to the activation energy of polyP hydrolysis in neutral solutions, which exceeds 104 kJ·mol^{-1}.[59]

In nature, in the living world, polyP is found from bacteria to humans.[2,48] Very long polyP chains are synthesized in bacteria and yeast, up to 1000 P_i residues. PolyP molecules in humans are mostly shorter. They occur both intra- and extracellularly with a chain length of 50 to 100 P_i units,[61] but also longer polyP chains of >500 P_i units are present.[62] In humans, polyP can be detected in almost all cells and tissues.[1,63] The polymer is enriched in the platelets, where it is stored in the dense granules (acidocalcisomes) and released into the extracellular fluids after platelet activation.[61,64] Comparatively, high concentrations of polyP are found in bone tissue, where the polymer has been shown to play an important role in mineralization, both as an energy donor and as a source of phosphate.[3,65–67]

Polyphosphate Metabolism

In contrast to bacteria, where polyP is synthesized from ATP (or GTP) by polyP kinases in a reversible reaction,[68] polyP anabolism in mammalian cells or human cells is not well understood. The main cell organelles involved in polyP formation and storage in mammalian/human cells are the mitochondria and the acidocalcisomes. While the function of mitochondria in polyP anabolism has been well demonstrated,[69,70] the ability of the acidocalcisomes to synthesize polyP has only been shown in yeast.[71] However, the acidocalcisomes are the main storage organelles of the polymer.[3,72] The mitochondrial polyP synthesis is driven by the energy of the gradient/potential at the inner mitochondrial membrane.[69,73] ATP formed by the F_OF_1-ATP synthase complex of the respiratory chain is used as substrate. Oligomycin, an inhibitor of the enzyme, suppresses polyP formation.[69] In yeast, acidocalcisomal polyP synthesis is mediated by the vacuolar transporter chaperone (Vtc) complex in the acidocalcisome membrane, which has polyP polymerase activity on its cytoplasmic side.[71]

Much more is known about the mammalian enzymes involved in polyP catabolism. PolyP hydrolysis is catalyzed by both exopolyphosphatases and endopolyphosphatases, which either split monomeric P_i from the ends of the polymer chain or

cleave the polymer in the middle of the chain.[63] The hydrolytic cleavage of the energy-rich phosphoanhydride bonds of polyP by both enzymes is exergonic. The chemical equilibrium is almost exclusively on the product side. In bacteria, polyP degradation can also proceed via the reversible reaction of the bacterial polyP kinases, which catalyze both the transfer of the γ-P_i from ATP to polyP (polyP synthesis) and the transfer of the terminal P_i from polyP to ADP.[48,74]

The major mammalian/human polyP-degrading enzyme is alkaline phosphatase (ALP), a ubiquitous enzyme with broad substrate specificity.[3,75] This enzyme, which is found both intra- and extracellularly at the plasma membrane, is able to catalyze the hydrolytic cleavage of phosphomonoester and phosphoanhydride bonds as present in AMP, ADP and ATP, β-glycerophosphate and polyP, including pyrophosphate (PP_i).[3,75,76]

Several tissue-specific isoforms of ALP are found in humans, including tissue-nonspecific ALP (bone, liver, and kidney), intestinal ALP, placental ALP, and germ cell ALP.[75,77] The ALP fraction present in human blood plasma is mainly the tissue-nonspecific ALP (TNAP),[78] a homodimer released from the outer cell membrane by cleavage of its glycosyl-phosphatidylinositol (GPI) anchor.[75]

The non-enzymatic, acid-catalyzed hydrolysis of polyP proceeds via formation of a pentavalent intermediate formed by nucleophilic attack of water at the ends of the molecule after protonation of the double-bond oxygen at the terminal P_i residues.[59,60] The molecular mechanism of the enzymatic, ALP-mediated hydrolysis of polyP (optimal at alkaline pH) is most likely similar to pyrophosphate hydrolysis, which involves (1) binding of the substrate and transfer of phosphate to a serine residue in the active site of the enzyme, and (2) hydrolysis of the enzyme-phosphate intermediate and the release of P_i by dissociation of the phosphate-enzyme complex.[75] The reaction could also proceed via the transient formation of a non-covalent enzyme-bound metaphosphate species, as proposed for the phosphate monoester hydrolysis by the enzyme.[79] This (negatively charged) metaphosphate intermediate is coordinated to two Zn^{2+} ions and a positively charged arginine residue, which are present at the catalytic site of ALP.

The ALP is a highly promiscuous enzyme,[80] which, in addition to the hydrolase activity, exhibits phosphotransferase activity.[3,76] This enzyme, in combination with a second enzyme, adenylate kinase (ADK), is also able to convert the chemical energy present in the phosphoanhydride bonds of polyP into metabolically useful energy in the form of ATP,[81] as described in below on the section on Polyphosphate and energy generation.

It has been shown that the hydrolytic degradation of polyP to P_i by ALP follows a processive mechanism.[76] This mechanism (degradation of polyP without dissociation of the enzyme-substrate complex after each catalytic cycle) could contribute to the high k_{cat}/K_m values of the enzyme, which are close to the diffusion limit of 1 $nM^{-1}{\cdot}s^{-1}$; eg for the intestinal ALP at pH 7.5 and $polyP_{77}$ as substrate, 5.4 $nM^{-1}{\cdot}s^{-1}$ (based on P_i).[76] The hydrolysis of polyP is associated with a large energy release (a multiple of $\Delta G^0 = -30.5$ $kJ{\cdot}mol^{-1}$ per phosphoanhydride bond, depending on the chain length of the polymer).[3]

The two other exopolyphosphatases identified in mammalian cells, the human metastasis regulator protein H-prune[82] and tartrate-resistant acid phosphatase,[83] only hydrolyze short-sized polyP molecules, in contrast to ALP, which degrades all size classes of polyP.[76] In addition to ALP, an exopolyphosphatase, a mammalian endopolyphosphatase has been isolated that degrades very long-chain polyP molecules into polymers with a size of 60 P_i residues.[84]

Coacervate Formation of Inorganic Polyphosphate

PolyP coacervates are mostly made from soluble polyP, eg, Na-polyP solutions, at neutral pH and room temperature; a stoichiometric ratio between phosphate and metal ion is usually used.[3] On the other hand, amorphous polyP nanoparticles are prepared from Na-polyP in the presence of excess amounts (overstoichiometric ratios) of metal ions compared to polyP (based on P_i) at alkaline pH (pH 10).

In addition to metal ions, polyP coacervates can be obtained by adding organic solvents, which have a lower dielectric constant than water, to aqueous Na-polyP solutions.[85–88] The metal ions used for coacervate formation include both monovalent (Na^+, Ag^+), divalent (Ca^{2+}, Mn^{2+}, Sr^{2+}, Zn^{2+}, Co^{2+}, Ni^{2+}) and trivalent cations (Fe^{3+}, Al^{3+}, and Eu^{3+}).[5,89–98] The more viscous and denser polyP coacervate phase obtained after phase separation predominantly comprises the longer polyP chains, while the less viscous supernatant mainly contains the shorter polyP chains.[98,99] PolyP coacervates are highly hydrated with a water content of up to 80%, eg, for the Al-polyP coacervate.[100] A high water content of about 40% of the coacervate weight has also been reported for the Ca-polyP coacervates.[96]

The viscosity of the polyP coacervates depends on the chain length of the polymers and the type of divalent cation,[97] as well as on the molar ratio of the metal ion and polyP (based on P_i).[96] Coacervates formed from polyP and Sr^{2+} or Ba^{2+} ions have a higher density than the Ca-polyP coacervate, which is attributed to the higher atomic mass of these elements and a lower water content.[96]

In addition, it was found that the viscosity of sodium polyP coacervates obtained by adding methanol to a Na-polyP solution[88] increases with decreasing dielectric constant of the solution (increase of the molar fraction of the added methanol).[88] PolyP coacervates have also been prepared by adding methanol to Ni-polyP and Co-polyP formed by direct mixing of a Na-polyP solution and a solution of the metal chlorides in a 2:1 molar ratio between phosphorus and metal ion (Ni^{2+} or Co^{2+}).[87] However, the most commonly used method to produce polyP coacervates is to slowly add the metal ion to the polyP solution with stirring at room temperature.[5,95,96] Using these conditions, the addition of the organic solvent is not necessary.

The mechanism of the polyP coacervation process is not fully understood. Coacervate formation is obviously driven by several forces, some of which act in opposite ways, such as electrostatic repulsion and van der Waals attraction. Electrostatic repulsion between the highly negatively charged polyP molecules and the higher entropy for polyP in solution than for the polymer within the coacervate counteracts phase separation, while the hydrophobicity of the dense phase and the ion pairs formed between the positively charged counterions and the negatively charged phosphate groups support coacervate formation.[95,101] It is conceivable that the addition of positively charged metal ions to a Na-polyP solution induces phase separation by shielding the negative charges on the polyP chains, thus reducing Coulomb repulsion; in addition, attractive forces due to the formation of hydrophobic metal-phosphate complexes, as suggested by Momeni and Filiaggi,[95] combined with entropic effects support polyP coacervate formation.

Experimental evidence has been presented that polyP has two types of binding sites for metal ions, "cage"-like binding sites that are used at low metal ion concentrations (high phosphate/metal ratio) and binding sites on the polymer surface.[92] This conclusion has been drawn on the basis of studies on the interaction of polyP in solution with Ca^{2+} and Eu^{3+} ions using FTIR, Eu^{3+} luminescence, and ^{31}P NMR spectroscopy.[92] It is assumed that saturation of the cage-like sites at higher metal ion concentrations leads to binding of the metal ions to the second type of binding sites that allows cross-links with adjacent polyP chains. Metal ions bound at the cage-like binding sites are shielded by the surrounding polyP phosphate groups, which prevent or interfere with the interaction of the metal ions with the water molecules.

These results were corroborated by results from extended X-ray absorption fine structure spectroscopy (EXAFS) analysis and Raman spectroscopy.[87] In these studies, coacervate formation between polyP and the transition metal ions Ni^{2+} and Co^{2+} was investigated. Again, two distinct phases of polyP coacervate formation could be distinguished. The EXAFS studies showed that each metal ion is surrounded by two phosphorus atoms. The structural disorder depends on the concentration of the metal ion. Two different P–O bonds can be distinguished in the polyP chain; a bridging P–O bond involved in linking the P_i units forming the polyP chain and terminal P–O bonds pointing outwards from the polyP chain. Analysis of the Raman spectra for symmetric stretching vibrations of the bridging P–O bonds and the terminal P–O bonds revealed that the strengths of these bonds change differently during the addition of the metal ions, indicating the existence of two distinct phases in the course of coacervation.[87] The results showed that at low metal ion concentrations (phosphorus/metal ratio higher than 6), but not at higher metal ion concentrations (phosphorus/metal ratio between 2 and 6), the strength of the terminal P–O decreases and the strength of the bridging P–O bond increases. It was concluded that as the concentration increases, the metal ions first bind to the cage-like binding sites within the polyP chain and then to further binding sites that allow the metal ions to join adjacent polyP chains, leading to coacervate formation.[87] As the metal ions bound outside of the cage-like sites become more exposed to water molecules, the electronic density of the metal-oxygen bonds decreases, resulting in an increase in the strengths of the terminal P–O and bridging P–O bonds.

Based on this knowledge, the following hypothetical scheme for the polyP coacervate formation in the presence of divalent cations can be proposed (Figure 2). According to this scheme, two phases during polyP coacervate formation are distinguished that are passed through with increasing concentrations of the divalent cation. In aqueous solution, the polyP chains of soluble polyP salts, eg, Na-polyP, do not aggregate due to Coulomb repulsion of the polyanionic polymers. Addition of small amounts of divalent cations, eg, Ca^{2+} ions, leads to complexation of these metal ions, whereby these ions occupy "cage"-like metal-binding sites within the polymer.[92] This process is associated with an increase in enthalpy

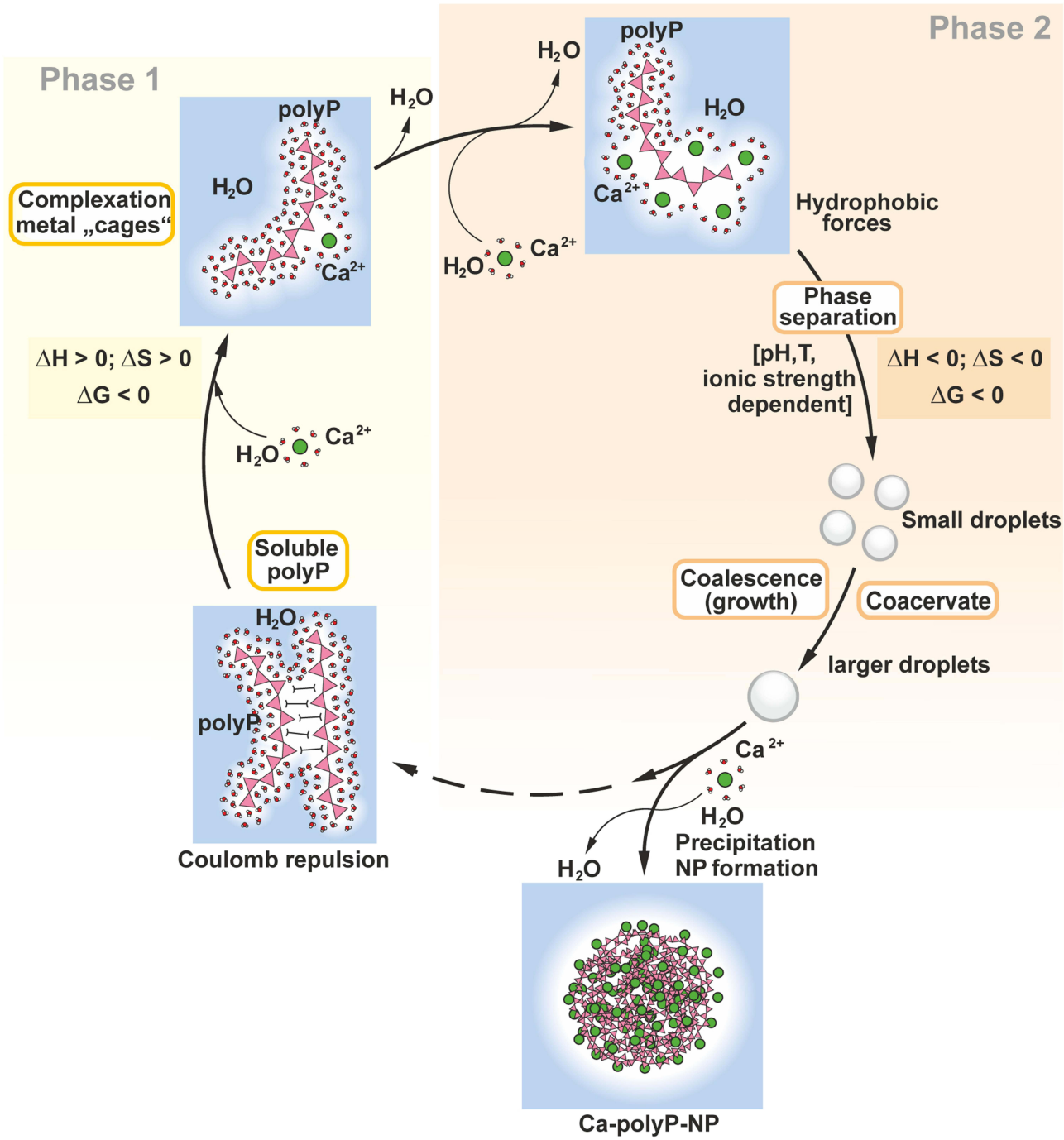

Figure 2 Proposed steps for polyP coacervation in the presence of divalent cations; schematic presentation. The first phase of polyP coacervate formation (Phase 1; addition of small amounts of divalent cations, eg, Ca^{2+} ions), leading to occupation of "cage"-like metal binding sites, is associated with an increase in enthalpy and entropy due to the loss of water molecules from the hydrate layers and the decrease in solvation energy. ΔG is negative, since $|\Delta H| < |T \cdot \Delta S|$ (absolute values). The second phase of coacervate formation (Phase 2; increasing amounts of divalent cation) is associated with a negative change in enthalpy (hydrophobic interaction) and entropy (increasing order of the surrounding water molecules). ΔG is negative, since $|\Delta H| > |T \cdot \Delta S|$. The formation of hydrophobic areas on the polyP molecules (hydrophobic interactions due to charge neutralization) and continuing water expulsion finally leads to phase separation and formation of small and the larger droplets. Ca-polyP nanoparticles (Ca-polyP-NP) are obtained in the presence of excess amounts of Ca^{2+} ions at alkaline pH.

and entropy due to the loss of water molecules in the hydrate layers of the metal ions and around the interconnected P_i residues of the polyP (positive ΔH and ΔS), and the decrease in solvation energy. Since $|\Delta H|$ is smaller than $|T \cdot \Delta S|$ for metal complexation of polyP (see below),[102] ΔG is negative (Phase 1). A further increase in the amount of divalent cation leads to the binding to further binding sites on the polyP molecule. The resulting neutralization of the negative charges on

the polyP chain by the positively charged metal ions leads to the formation of hydrophobic areas on the polyP molecules and expulsion of more water molecules, resulting in hydrophobic interaction between these polymers and finally to phase separation to form a still water-rich coacervate. This second phase of the coacervation process (Phase 2) is associated with a negative change in enthalpy (due to hydrophobic interaction) and entropy (increasing order of the surrounding water molecules). ΔG is negative since |ΔH| is greater than |T·ΔS|. First small droplets form, which coalesce into larger drops. Addition of excess amounts of Ca^{2+} ions, particularly at alkaline pH values, can finally lead to the formation of Ca-polyP nanoparticles.

This model is also supported by turbidity measurements,[95] which showed that coacervate formation of soluble polyP with Ca^{2+} ions occurs above a critical ratio between calcium and polyP (based on P_i); during the addition of Ca^{2+} ions to the Na-polyP solution, the hydrophobic forces steadily increase and the electrostatic repulsion of the polyanionic polyP chains steadily decreases due to complexation of Ca^{2+} by two PO_3^- units of the polyP chain until this ratio is reached; then phase separation occurs. This critical Ca: P ratio is getting smaller with increasing concentrations of Na-polyP. The latter effect has been attributed to an increased entropy difference between polyP in solution and polyP entrapped in the coacervate at low Na-polyP concentration compared to Na-polyP at high concentrations of the polymer.[95] In general, polyP in solution has a higher level of entropy than polyP in the coacervate. This negative entropy contribution (negative entropy change) must be compensated and exceeded by the contributions of hydrophobic and other forces. Therefore, at low Na-polyP concentrations, an increased Ca: P ratio is required for phase separation to occur.

Thermodynamic data on complex formation between polyP and metal ions, which is the first step in metal ion-induced polyP coacervate formation occurring before phase separation, are available. The ΔG^0 for the complex formation of Ca^{2+} with longer-chain polyP is −42.7 kJ·mol^{-1}.[103] The corresponding enthalpy (ΔH^0) is 4.2 kJ·mol^{-1}.[103] Therefore, the complexation of the metal ion with polyP is associated with a positive change of entropy (ΔS^0). This change in entropy is due to the altered hydration of the ion and the involved P_i groups of the polyP molecule, ie, the release of water upon binding of the metal ion to polyP.[103] More detailed thermodynamic data reported by Sugano and Kubo,[102] showing that ΔH^0 for the formation of a 1:1 complex with $polyP_8$ (chain lengths, 8 P_i units) decreases with increasing radius of the metal ion from 20.9 kJ·mol^{-1} (Mg^{2+}) to 14.2 kJ·mol^{-1} (Ca^{2+}) and 13.8 kJ·mol^{-1} (Sr^{2+}). Similarly, ΔS^0 decreases in the order 0.25 kJ·K^{-1}·mol^{-1} (Mg^{2+}), 0.21 kJ·K^{-1}·mol^{-1} (Ca^{2+}) and 0.20 kJ·K^{-1}·mol^{-1} (Sr^{2+}), resulting in a reduction of the absolute values for ΔG^0, which changed from −54.4 kJ·mol^{-1} (Mg^{2+}) via −48.1 kJ·mol^{-1} (Ca^{2+}) to −44.4 kJ·mol^{-1} (Sr^{2+}).

Recently, in silico simulation studies have been performed to investigate the molecular interactions between the three components involved in the pH-dependent Ca-polyP coacervate and Ca-polyP nanoparticle formation – polyP, Ca^{2+}, and water molecules. Surprisingly, these studies showed different changes in the distribution of polyP and calcium ions during the reaction.[104] Under conditions that support coacervate formation, these components show a more or less random arrangement pattern, while nanoparticle formation is characterized by clustering of the anionic polyP molecules accompanied by partial separation of the Ca^{2+} cations. These results made it possible to propose a model of Ca-polyP coacervate and nanoparticle formation that also takes into account ion–dipole interactions in addition to electrostatic interactions.[104] It is proposed that at pH 7 the initially randomly organized Ca^{2+} and polyP ions, surrounded with a hydrate shell, assemble in a time-dependent manner into concentric ring-like structures with a polyP core and outer Ca^{2+} ions forming liquid droplets that coalesce, to form a water-rich coacervate. At pH 10, compartmentalization takes place and significantly denser structures form,[104] caused by the higher negative charge and Ca^{2+} binding affinity of the almost completely ionized polyP molecule, which also applies to the second, less acidic OH of its P_i end groups.[95,105]

Turbidimetric measurements showed that Ca-polyP coacervate formation at pH 7 is a slow process compared to nanoparticle formation at pH 10.[104] The formation of the respective products could be confirmed not only by SEM but also by FTIR measurements. It was found that the coacervate and the nanoparticles of Ca-polyP show a characteristic difference in their FTIR spectra, which allows a distinction between the two Ca-polyP phases. The $\nu_{as}(PO_2)^-$ signal at a wavenumber of 1255 cm^{-1}, which forms a distinct peak in the spectrum of the Ca-polyP coacervate, is absent and remains only as a shoulder in the spectrum of the Ca-polyP nanoparticles.[104] This signal has been attributed to the asymmetric stretching vibrations of the internal $(PO_2)^-$ units of the polyP chain. This change in the FTIR spectrum is believed to be caused by the binding of Ca^{2+} at the internal P_i residues of the polyP chain. Interestingly, the formation of a coacervate or nanoparticles depends on the way the two components, polyP and Ca^{2+} ions, are combined. In the

conventional procedure, by slowly adding a $CaCl_2$ solution to a Na-polyP solution, coacervation is observed at pH 7 and nanoparticle formation at pH 10. If, however, the Na-polyP solution is dropped into the $CaCl_2$ solution, a coacervate is obtained at both pH values.[104] Under these conditions, the $\nu_{as}(PO_3)^{2-}$ signal does not disappear as it does during the formation of the nanoparticles. This finding is explained by an immediate binding of Ca^{2+} ions to polyP when dropping the Na-polyP into a $CaCl_2$ solution containing excess amounts of the divalent cation (2.5-fold on the stoichiometric basis of Ca: P).

Coacervate formation of polyanionic polyP induced by metal ions (cations) and possibly proteins such as surface-associated proteins can result in the encasement/encapsulation of bacteria, viruses and cells (Figure 3A), as shown, for example, for the corona virus SARS-CoV-2.[106] As a result, the deleterious effects of pathogens are mitigated or prevented. This could be particularly relevant in wound therapy. Bacterial infection is an important factor leading to the development of chronic wounds. We could show that soluble Na-polyP and Ca-polyP nanoparticles incorporated into a hydrogel matrix are converted into the physiologically active coacervate upon contact with protein-containing wound fluid leading to the entrapment and killing of bacteria, while maintaining normal cell function.[107] In particular, the formed polyP coacervate can counteract cell damage caused by bacterial α-toxin (hemolysin A), a pore-forming protein secreted by these organisms[108] that is inserted into the cell membrane, leading to efflux of intracellular ATP[109] and cell death.[110] ATP formed from polyP in the extracellular space by the combined action of membrane-bound ALP and ADK[81] can block the release of cellular ATP through the α-hemolysin pores. The bacteria entrapped in the polyP coacervate are

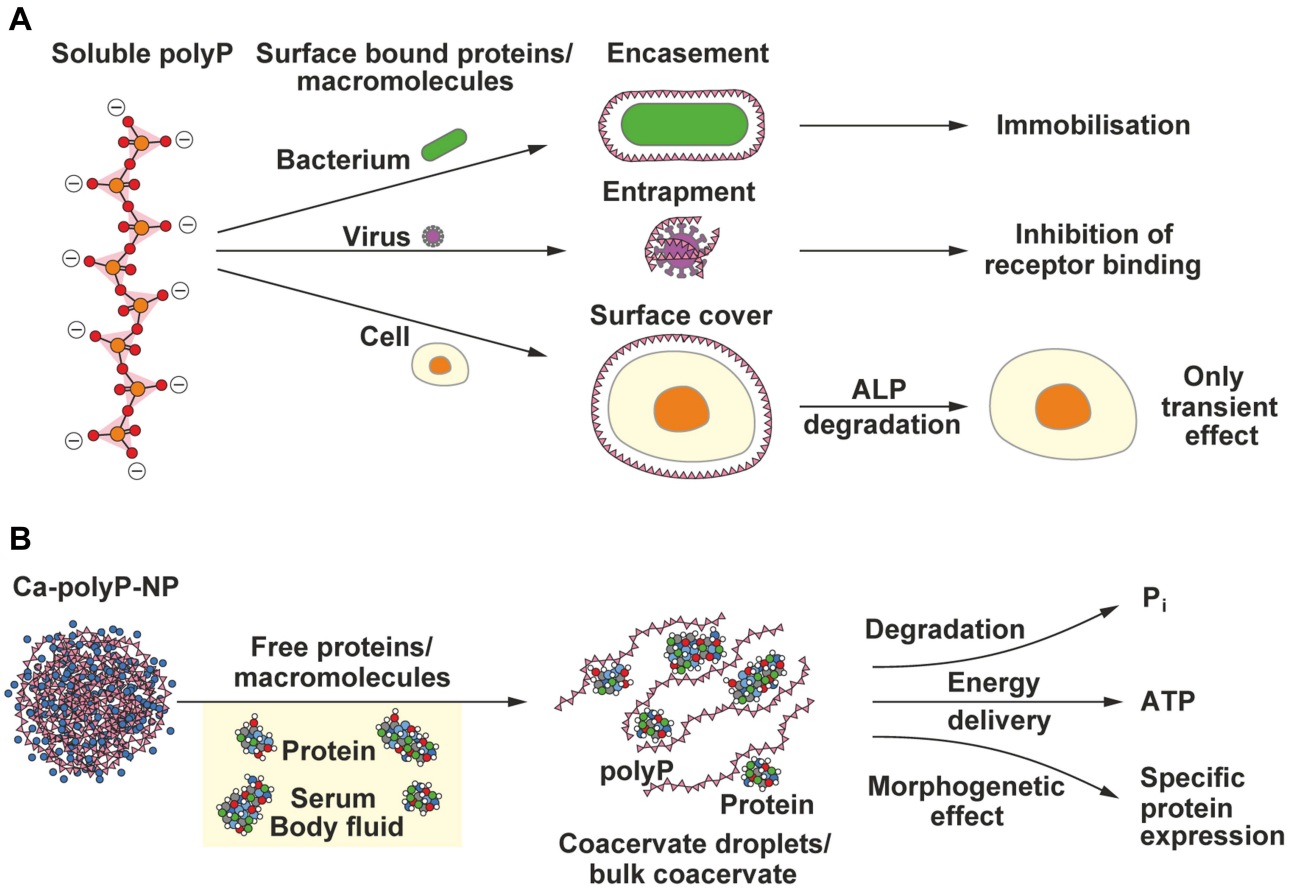

Figure 3 Coacervate formation of the polyanionic polyP induced by positively charged surface-bound or soluble proteins/macromolecules and biological effects. (**A**) Encasement/entrapment of bacteria, viruses and cells by forming a polyP coacervate upon contact with surface-associated proteins, leading to immobilization and functional impairment (bacteria and cells) or inhibition of receptor binding (viruses). The inhibitory effect of the surface cover formed by the coacervate could be transient, eg, as a result of degradation of polyP by cell-surface-bound alkaline phosphatase (ALP; can also be present on bacterial surfaces). (**B**) Coacervate formation upon contact of polyP nanoparticles (depot form), eg, Ca-polyP nanoparticles, with free, soluble proteins as present, eg, in blood serum and other body fluids. Only after conversion into the coacervate does polyP become degradable (via ALP) and biologically active, supplying metabolic energy (ATP) and exhibiting morphogenetic activity (induction of specific gene expression).

most likely killed by chelation of Ca^{2+} ions.[111] The coacervate layers formed on cells presumably exist only transiently due to hydrolysis of the polymer by cell-surface-bound ALP.

In addition to extracellular generation of ATP, the cellular uptake of polyP nanoparticles[112] can contribute to balancing the loss of the intracellular ATP, providing the metabolic energy needed for wound healing. Also intracellularly, polyP has been shown to cause coacervate formation by interaction with positively charged proteins, as demonstrated in experiments with green fluorescent protein.[113]

Properties of Polyphosphate Coacervates versus Polyphosphate Nanoparticles

In nature, but also synthetically, amorphous nano- or microparticles of polyP can serve as a storage form of the polymer. These particles are deposited in the acidocalcisomes, particularly in the platelet dense granules.[62,64,114,115] They are also found on the platelet surface after activation.[116] In order to synthesize amorphous polyP particles, we have developed a biomimetic procedure.[49] The amorphous character of these particles is important for their biological activity. Only in the amorphous form are polyP nano/microparticles biologically active. In this property they are similar to phosphate-based materials presently used in bone tissue engineering, eg crystalline hydroxyapatite, have proven to be significantly less active compared to preparations composed of amorphous phosphate.[53] However, the polyP in the amorphous nano/microparticles is not immediately active but needs to be converted to the coacervate phase in order to become bioavailable and biodegradable and to exhibit its morphogenetic and energy delivering activity.

PolyP nano- and microparticles have been prepared with different counterions, both divalent and trivalent cations, such as the alkaline earth metals Ca^{2+}, Mg^{2+} and Sr^{2+} or transition metals like Zn^{2+} or the rare-earth metal Gd^{3+}.[49,51,52,117,118] An aqueous solution of the metal salt (chloride, nitrate, etc.) is slowly added to an aqueous solution of Na-polyP while stirring at room temperature, the pH being kept constant in the alkaline range. A pH of 10 and a superstoichiometric metal/phosphate ratio (mostly 2:1) are usually used. Different chain length of polyP can be used, but polyP with an average size of 40 P_i units, close to the size of the physiological polyP, is preferred. The synthesized particles have a spherical morphology. They are amorphous, as can be confirmed by powder X-ray diffraction (XRD) analysis.[49,50,52] Depending on the preparation protocol, eg, by varying the drop rate or the concentration of the components or by fractionating the products by ultrafiltration, polyP nano/microparticles can be produced within a specific size range.[49,119]

The amorphous polyP nano/microparticles are characterized by a strongly negative zeta (ζ) potential (−33.6 mV for Ca-polyP nanoparticles).[5] This ζ potential is caused by a charge separation occurring when the particles are suspended in aqueous solution. Therefore, once suspended in protein-free aqueous solutions, the particles remain dispersed and do not tend to aggregate due to electrostatic repulsion. This strongly negative ζ potential is also a reason for the high stability of the particles in aqueous solvents at neutral or alkaline pH in the absence of protein. They can be stored for a long time when dried.

However, in order to become biologically active, these particles need to be converted to the coacervate state (Figure 3B). We have shown that after exposure to peptides or proteins or protein-containing fluids such as blood serum or wound exudate, the amorphous polyP particles, eg, Ca-polyP or Zn-polyP nanoparticles are transformed into the coacervate phase. Conversion of the polyP particles into the coacervate can also be induced by changing the pH to neutral or acidic values. The formed coacervate is less stable than the nanoparticles. The polyP molecules forming the coacervate are prone to degradation by ALP, leading to the disintegration of the coacervate droplets (Figure 3B). During this process, the polyP molecules become accessible and begin to develop their morphogenetic activity. Furthermore, when coupled with ADK (both ALP and ADK are attached the outer cell membrane), ALP acts as a donor of metabolic energy and provides ATP for the function and development of the extracellular matrix (ECM) (Figure 3B). As a result, increased proliferation of the cells growing on the coacervate and active migration of cells into the coacervate are observed.[5]

The transition of the polyP nanoparticles into the coacervate phase is associated with a reduction in the ζ potential of the particles (Figure 4A).[5] Incubation in PBS does not lead to any significant change in ζ potential. The SEM images in Figure 4 show the transformation of Ca-polyP nanoparticles into the coacervate phase after suspension and incubation in medium supplemented with fetal calf serum (Figure 4C) compared to protein-free medium (Figure 4B).[3]

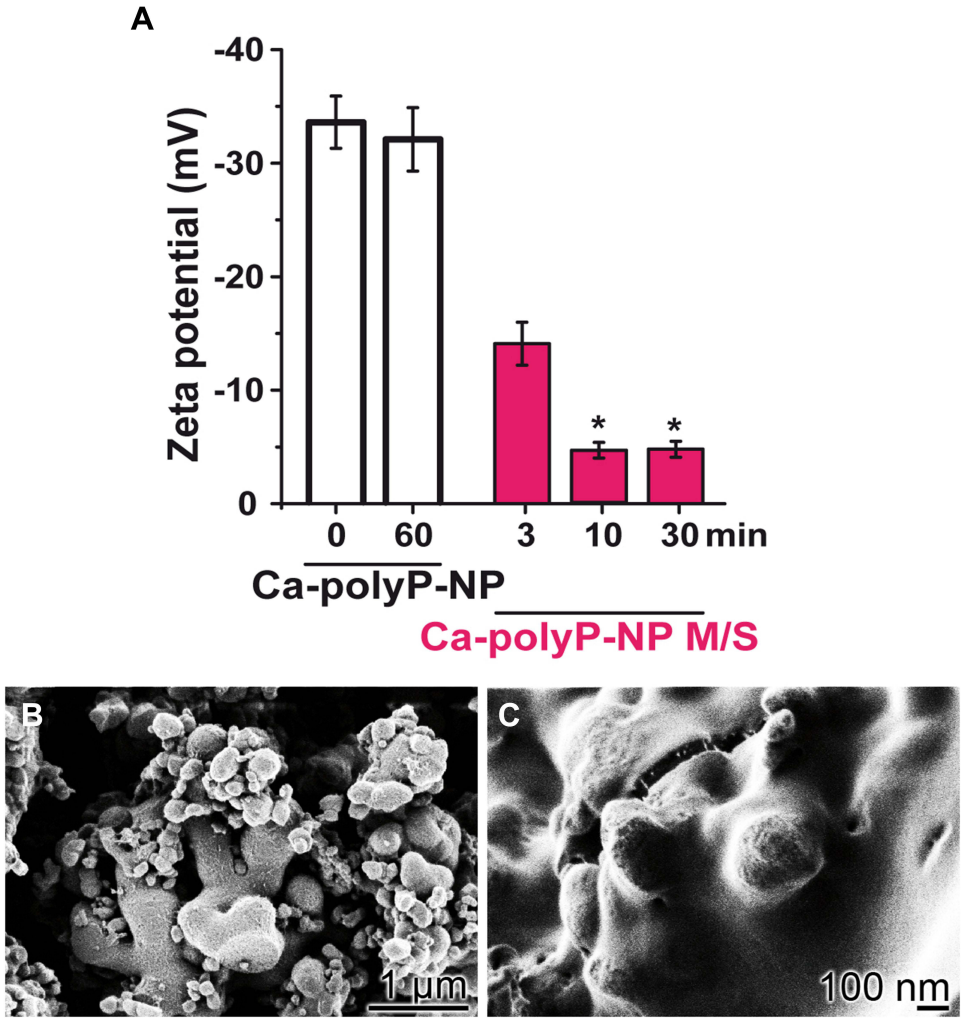

Figure 4 Changes in the zeta potential and in the morphology of Ca-polyP nanoparticles induced by protein exposure. (**A**) Zeta potential of the nanoparticles (Ca-polyP-NP) during incubation in phosphate-buffered saline (PBS; open bars) and in medium/serum (M/S; magenta bars). Only in the presence of protein (incubation in M/S) a marked drop of the zeta potential of the particles is observed, while the potential remains unchanged in PBS even during a 60 min incubation period. The means ± SD from 5 experiments are shown (*$p < 0.05$). (**B** and **C**) Morphology of the Ca-polyP nanoparticles after incubation in protein-free medium (**B**) and after incubation in medium containing 10% fetal calf serum (**C**). High resolution SEM images. Adapted with permission from Müller WEG, Wang SF, Tolba E, et al. Transformation of amorphous polyphosphate nanoparticles into coacervate complexes: an approach for the encapsulation of mesenchymal stem cells. Small. 2018;14(27):e1801170. © 2018 Wiley-VCH Verlag GmbH & Co. KGaA, Weinheim.[5]

Accordingly, polyP coacervates form an adaptable matrix that mimics a stem cell niche.[120] They are able to provide the metabolic signals and metabolic energy needed to induce cell growth and differentiation and promote tissue repair.[3] In addition, as a potential implant material, they are cell-attracting and support the ingrowth of cells, eg, human mesenchymal stem cells (MSC), which are embedded in this matrix.[5]

The formation of Ca-polyP nanoparticles in alkaline aqueous solution and the presence of excess amounts of Ca^{2+} ions compared to polyP (based on P_i) is associated with a drastic size reduction and expulsion of water (syneresis) compared to the water-rich coacervate (Figure 5A). It is proposed that the formation of additional negatively charged oxygens at alkaline pH through dissociation of the second OH group at the ends of the polyP chains allows the formation of Ca^{2+} bridges, leading to contraction of the Ca-polyP structure and expulsion of water (Figure 5B). The porous structure of the Ca-polyP nanoparticles allowing the draining of liquid and visible in electron micrographs (Figure 4B) is thought to be due to the repulsion of Ca^{2+} ions located on the surface of opposing polyP strands (Figure 5B). The larger Ca^{2+} concentration needed for Ca-polyP nanoparticle formation compared to coacervate formation can result in the

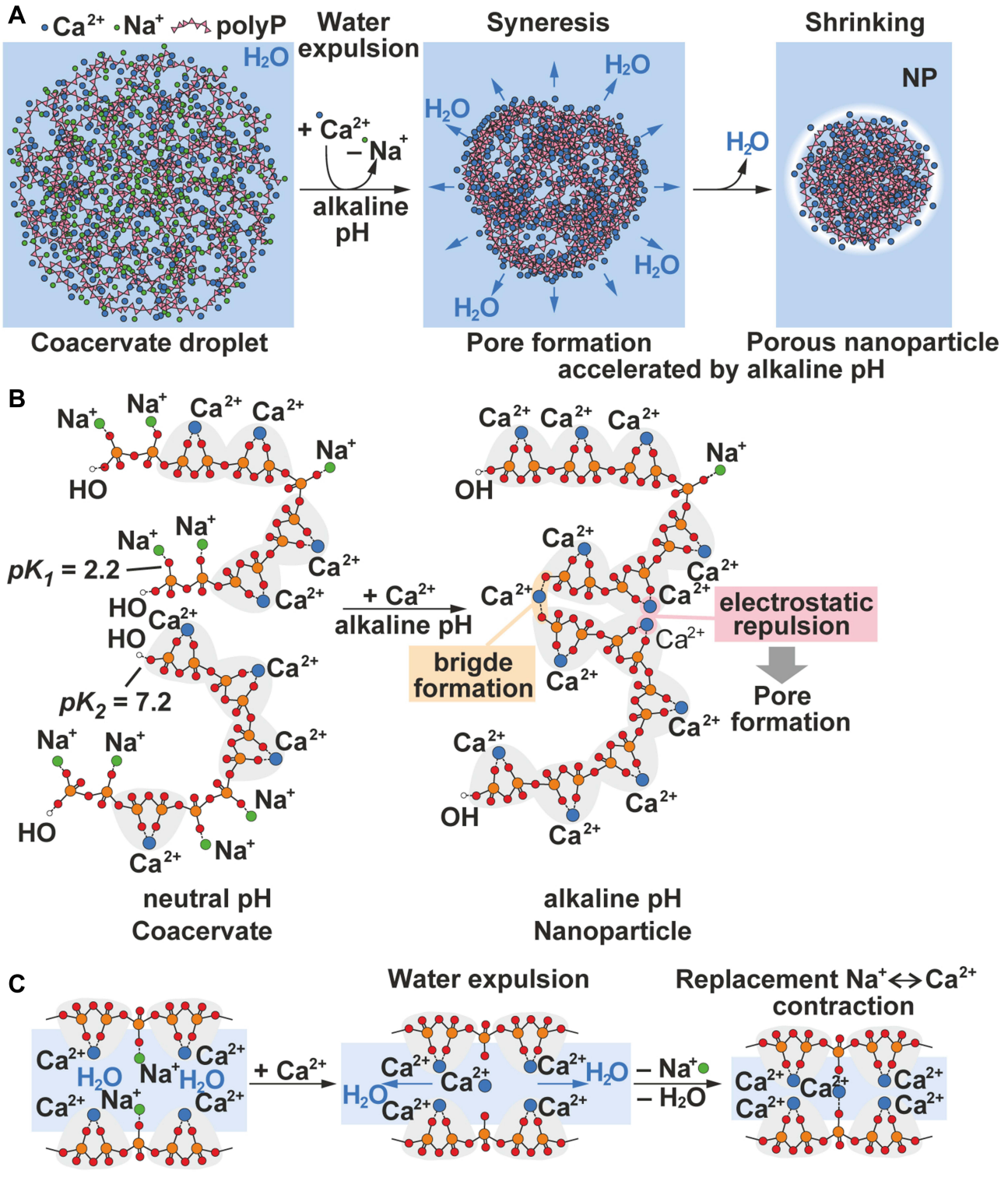

Figure 5 Proposed mechanism of pore formation during nanoparticle formation from Ca-polyP coacervate. (**A**) Phase transition of a Ca-polyP coacervate droplet consisting of polyP, Ca^{2+} and Na^{+} ions into a porous Ca-polyP nanoparticle (NP) by alkalization and addition of further Ca^{2+} ions. This process is associated with expulsion of water (syneresis), release of residual Na^{+} (from the preparation procedure) and shrinkage. (**B**) At neutral pH, the internal and first terminal OH groups of the polyP chains within the coacervate are almost completely dissociated (pK_1 = 2.2), while the second terminal OH is only about 50% dissociated (pK_2 = 7.2). Each Ca^{2+} ion is bound to two phosphate units while Na^{+} is bound to the remaining phosphate units. In addition, Ca^{2+} bridges formed between phosphate units of two individual polyP chains can occur (not shown). Increasing the pH leads to dissociation of the second terminal OH group, allowing Ca^{2+} bridging between the ends of two polyP strands. The consequence is a contraction of the structure, which leads to expulsion of water. The electrostatic repulsion between opposing Ca^{2+} ions bound to the surface of adjacent polyP chains creates pores that are used for water exfiltration. (**C**) Addition of more Ca^{2+} ions (increasing the Ca: P ratio) leads to the replacement of Na^{+} ions by Ca^{2+} ions that form bridges between adjacent polyP strands.

formation of additional Ca^{2+} bridges between adjacent polyP strands, accompanied by a release of Na^{+} ions as the result of a Na^{+}/Ca^{2+} exchange (Figure 5C).

Polyphosphate Coacervates in Tissue Engineering Scaffolds

Coacervate formation of polyP is essential for the morphogenetic and energy delivering activity of a variety of biohybrid materials formed from polyP or polyP nanoparticles and a variety of hydrogel-forming polymers. PolyP-containing hydrogel scaffold materials have been prepared by combining the polymer with other polyanionic polymers such as alginate, hyaluronic acid or *N,O*-carboxymethylchitosan, a carboxymethylated chitosan derivative, all of which are negatively charged at physiologically pH due to their multiple carboxyl groups.[50,121–124] These hybrid materials are hardened by adding divalent cations such as Ca^{2+} or Mg^{2+}, which lead to the formation of metal bridges between the polymers.

PolyP coacervates can either be generated directly during preparation of the scaffold materials, or these materials can be supplemented with amorphous polyP nanoparticles, which upon protein contact, eg, blood serum contact, are transformed into the coacervate phase. Alternatively, the nanoparticles such as Ca-polyP nanoparticles can be generated in situ. For example, the negatively charged polysaccharide karaya gum, poly(vinyl alcohol) (PVA), polyP and Ca^{2+} ions form a porous hybrid cryogel through Ca^{2+}-mediated ionic gelation of the gum and intermolecular cross-linking of PVA by freeze-thawing;[124] Figure 6A. Addition of Ca^{2+} ions leads to the in situ formation of 100−150 nm Ca-polyP nanoparticles (Figure 6B [left] and 6C). Upon contact with medium/serum, the nanoparticles within the cryogel are converted into a coacervate (Figure 6B [middle] and 6D). The formed polyP coacervate turned out to be a suitable matrix to attract stem cells (human MSC) and to support the adherence and invasion of MSC into the scaffold (Figure 6B [right] and 6E). It is assumed that the migration of the cells into the cryogel after polyP-coacervate formation is enabled by breakage of the ionic and hydrogen bonds between the polymers, mediated by cellular enzymes or due to pH changes.[124] Animal experiments showed that implantation of polyP/karaya gum/PVA-containing microspheres in rat muscle resulted in the formation of initial granulation tissue that was not seen in controls and led to the replacement of the implant material after 2−4 weeks.[124]

Another example for a polyP-containing hydrogel scaffold, which is activated by forming a coacervate upon contact with body fluids, is based on a combination of polyP with *N,O*-carboxymethylchitosan (*N,O*-CMC) and alginate. It was found that the polyP/*N,O*-CMC/alginate hydrogel matrix hardens through the formation of Ca^{2+} crosslinks between the polymers in the presence of Ca^{2+}ions.[121,122] This material could also be used as a bio-ink for 3D-printing of hydrogel scaffolds that even contain cells and support cell differentiation and proliferation. Recently, a *N,O*-CMC/alginate-based bio-ink was formulated, supplemented with both soluble Na-polyP and Ca-polyP nanoparticles; in addition, gelatin was added as a cell adhesion matrix (Figure 7A).[125] This bio-ink was suitable for 3D bio-printing of living cells such as MSC (Figure 7B). Exposure of the 3D-printed scaffold to medium/serum resulted in coacervate formation (Figure 7C), starting with the readily available soluble polyP (Na-polyP) and continuing with the Ca-polyP nanoparticles (depot form; Figure 7D) formed from the soluble Na-polyP after addition of Ca^{2+} ions. The formed polyP coacervate (Figure 7E) efficiently supported cell survival/proliferation due to its energy-providing and morphogenetic activities and promoted the attachment and ingrowth of MSC and their differentiation into mature, mineral-depositing osteoblasts.[125]

Materials based on polyP-coacervate or materials containing soluble polyP or stable polyP nanoparticles that are converted into a biologically active polyP-coacervate upon contact with proteinaceous body fluids have also been used for wound healing. Wound healing is a highly energy-dependent process[126] that is impaired under pathological conditions associated with insufficient oxygen or nutrient supply. These conditions can lead to the development of non-healing, chronic wounds that resist conventional therapy, such as diabetic, venous, arterial and pressure ulcers. The energy demand of the recovery zone during wound healing is required not only for energy-dependent cell migration, proliferation, and differentiation, but also the resynthesis, organization, and maintenance of the ECM surrounding the cells. Physiologically, this energy is provided by the platelets, which release polyP at the injured site after activation.[3,61,127] The supply of energy in the form of polyP is particularly important for the regeneration of the epidermis, since this non-vascularized skin layer depends on the supply of nutrients from the underlying dermis. PolyP serves as a source of

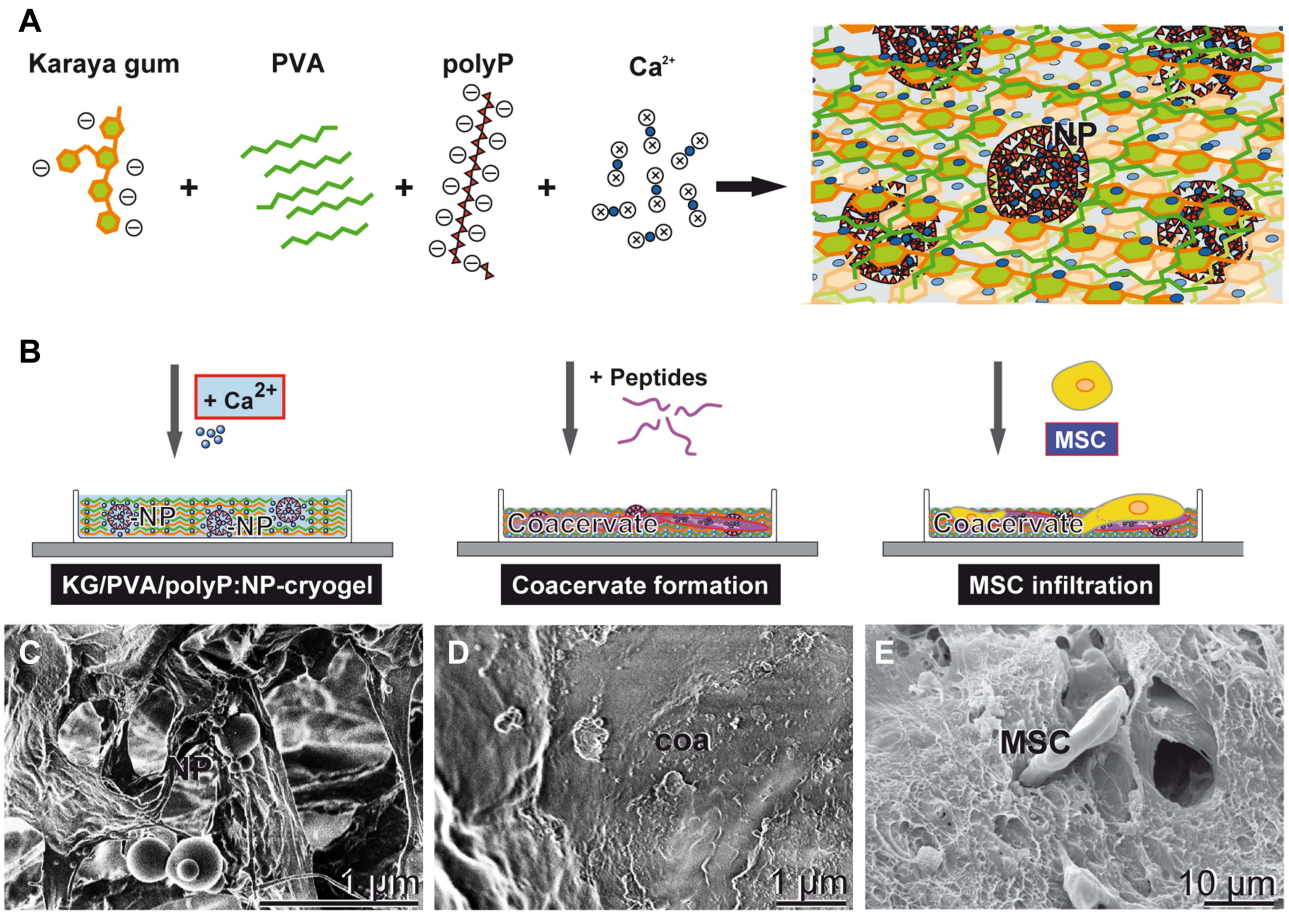

Figure 6 In situ nanoparticle formation and coacervation in a Karaya gum/poly(vinyl alcohol) (PVA)/polyP-cryogel. (**A**) Sketch of formation of the cryogel by physically cross-linking of PVA and ionic gelation of Karaya gum and Na-polyP (upper row). Ca^{2+} induces the cross-linking of Karaya gum as well as the in-situ formation of Ca-polyP nanoparticles (NP) with a size of 100–150 nm (KG/PVA/polyP: NP-cryogel; (**B** [left]). Exposure of the Ca-polyP-NP containing cryogel to medium/serum leads to transformation of the nanoparticles into a coacervate (**B** [middle]). The coacervate formed is a suitable matrix supporting the adherence and the infiltration of human mesenchymal stem cells (MSC) into the cryogel (**B** [right]). (**C**) KG/PVA/polyP: NP-cryogel with the in-situ formed nanoparticles (NP). (**D**) Coacervate (coa) formed after medium/serum exposure of KG/PVA/polyP: NP-cryogel. (**E**) Attachment and migration of MSC into the polyP-containing cryogel after coacervation. SEM images. Adapted from Tolba E, Wang XH, Ackermann M, et al. In situ polyphosphate nanoparticle formation in hybrid poly(vinyl alcohol)/karaya gum hydrogels: A porous scaffold inducing infiltration of mesenchymal stem cells. Adv Sci (Weinh). 2018;6(2):1,801,452. © 2018 The Authors. Published by WILEY-VCH Verlag GmbH & Co. KGaA, Weinheim. This is an open access article distributed under the terms of the Creative Commons CC BY license (https://creativecommons.org/licenses/by/4.0/).[124]

metabolic energy by providing ATP via the combined action of the two enzymes, ALP and ADK, both intra- and extracellularly.[3,81] Both enzymes are present in the wound bed.[107]

Both a wound repair gel and a wound mat with water-soluble polyP or stable polyP nanoparticles have been developed to support the healing of chronic wounds. The combination of polyP with hydrogel-forming polymers enabled the fabrication of biomimetic water-rich polymer networks that mimic the ECM in native tissues. These hydrogel networks provide a suitable, adaptable matrix that allows the embedded cells to migrate, proliferate and differentiate. The preparation of such a hydrogel matrix, consisting of polyP and an alginate and periodate-oxidized alginate network cross-linked via Zn^{2+} ions and gelatin via Schiff base formation, has been reported (Figure 8A).[128]

Cross-linking of alginate with divalent cations leads to the formation of a hydrogel matrix that is too rigid to allow sufficient cell migration. Therefore, a partially oxidized alginate matrix was used. Sodium metaperiodate served as oxidizing agent. During oxidation, the OH groups at C2 and C3 of the sugar-building blocks of alginate, a copolymer of 1,4-linked β-D-mannuronic acid and α-L-guluronic acid, are converted into aldehyde groups that can react with protein amino groups such as the ε-amino groups of lysine and hydroxylysine of gelatin, leading to formation of a Schiff base.[129]

PolyP was incorporated into this matrix, consisting of an ionically cross-linked unmodified alginate–modified (oxidized) alginate–gelatin hydrogel mesh, either in a depot form as solid Zn-polyP nanoparticles (prepared at pH 10),

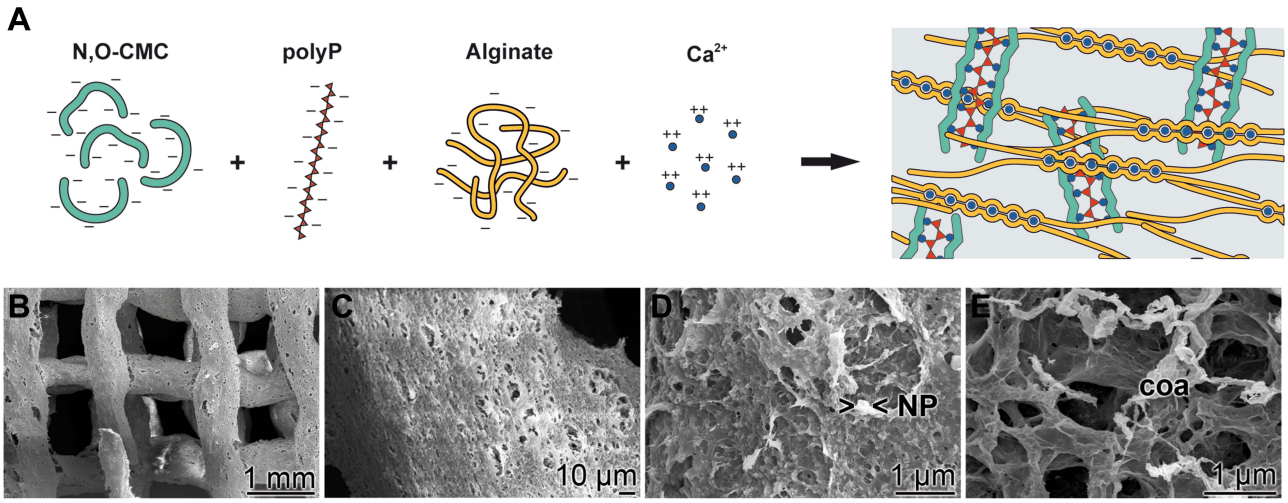

Figure 7 Coacervate formation within the polyP-based bio-ink for 3D printing. (**A**) Formation of the bio-ink from *N,O*-carboxymethylchitosan (N,O-CMC), polyP, alginate and Ca^{2+}. Additionally, gelatin is added to provide the hydrogel with a substrate for cell adhesion (not shown). (**B**) 3D-printed grid using the bio-ink. (**C**) Higher magnification of the grid after incubating in medium/serum. (**D** and **E**) During exposure to medium/serum, the Ca-polyP nanoparticles (NP; > <) (**D**), which are formed from soluble Na-polyP after addition of Ca^{2+} ions and act as a depot form of polyP, are transformed into the coacervate (coa) phase (**E**); ESEM. The polyP component of the bio-ink delivers the metabolic energy needed for the cells to grow and remain functionally active on the 3D-printed scaffold. Adapted from Neufurth M, Wang SF, Schröder HC, Al-Nawas B, Wang XH, Müller WEG. 3D bioprinting of tissue units with mesenchymal stem cells, retaining their proliferative and differentiating potential, in polyphosphate-containing bio-ink. Biofabrication. 2021;14:015016. © 2021 The Author(s). Published by IOP Publishing Ltd. This article is licensed under a Creative Commons Attribution 4.0 license (https://creativecommons.org/licenses/by/4.0/).[125]

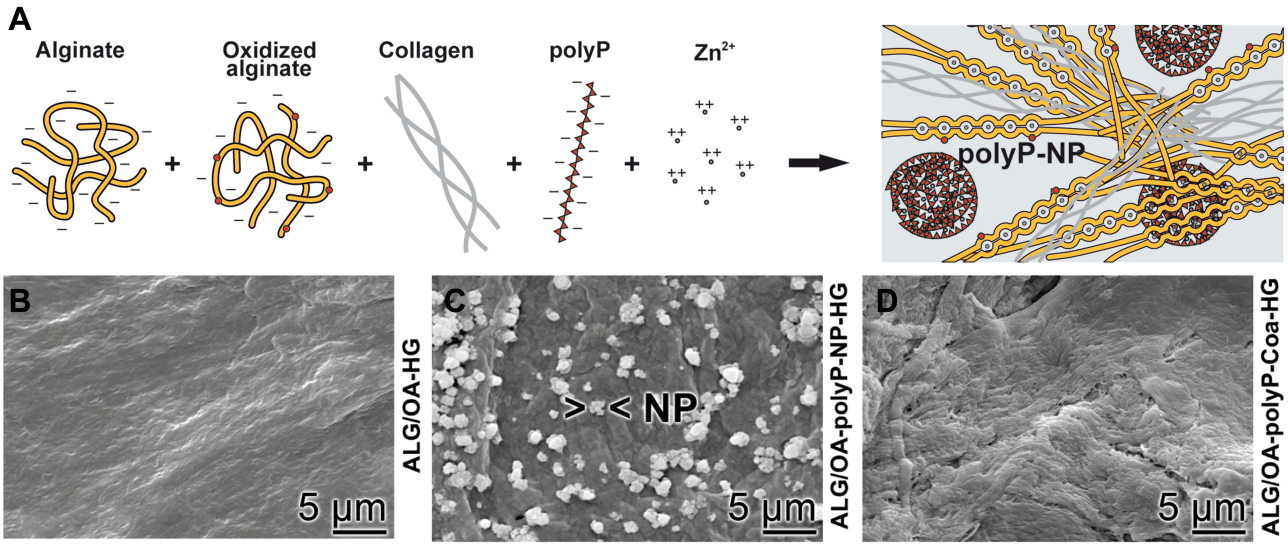

Figure 8 Preparation and surface morphology of an alginate/oxidized alginate hydrogel containing polyP nanoparticles or polyP coacervate. (**A**) Formation of the hydrogel from alginate, oxidized alginate, collagen, Na-polyP and Zn^{2+} ions. (**B**–**D**) Surface textures of the polyP-free hydrogel (ALG/OA-HG) (**B**) and of the Na-polyP-supplemented hydrogel treated with $ZnCl_2$ at alkaline pH ("ALG/OA-polyP-NP-HG") (**C**) or at neutral pH (ALG/OA-polyP-CoA-HG) (**D**); ESEM. After treatment with $ZnCl_2$ at pH 10 numerous Zn-polyP nanoparticles (NP; > <) are visible on the hydrogel surface (**C**), while at pH 7 a polyP coacervate is formed (**D**). Adapted from Wang SF, Wang XH, Neufurth M, et al. Biomimetic alginate/gelatin cross-linked hydrogels supplemented with polyphosphate for wound healing applications. Molecules. 2020;25(21):5210. © 2020 by the authors. Licensee MDPI, Basel, Switzerland. This article is an open access article distributed under the terms and conditions of the Creative Commons Attribution (CC BY) license (https://creativecommons.org/licenses/by/4.0/).[128]

which are converted into the biologically active coacervate phase after matrix exposure to protein at neutral pH, or directly as polyP coacervate that is immediately active.[128] Analysis of the morphology of the polyP-supplemented hydrogel matrix showed that the addition of Zn^{2+} ions to the hydrogel at alkaline pH (pH 10) leads to the in situ

generation of Zn-polyP nanoparticles (Figure 8C), while at neutral pH (pH 7) a polyP coacervate is formed (Figure 8D). For comparison, the hydrogel surface of the polyP-free hydrogel matrix is shown in Figure 8B.

In cell culture experiments with human epidermal keratinocytes, both the alginate–oxidized alginate–gelatin matrix supplemented with Zn-polyP nanoparticles after conversion of the particles in the coacervate phase and the Zn-polyP-coacervate-containing matrix strongly promoted the energy-dependent migration of the cells and cell attachment, spreading and cell growth compared to the matrix without the polymer.[128] Using a similar matrix, the potential of polyP to exhibit morphogenetic activity and to serve as a donor of metabolic energy was recently also demonstrated in vivo in patients suffering from chronic wounds that were refractory to conventional therapy.[107]

The collagen-based wound mat developed in addition to the wound gel consisted of amorphous Zn-polyP nanoparticles integrated into mechanically compressed collagen (Figure 9A).[118] The nanoparticles were embedded in the collagen mat during the compression process. After contact with wound exudate, they are converted into the biologically active polyP coacervate phase (Figure 9A and B). Only in the coacervate form is the polyP biodegradable and exerts its energy-supplying and morphogenetic activity. This coacervate supported the migration of cells from the granulation tissue of a chronic wound treated with the wound mat into the mat, as demonstrated in a wound biopsy specimen traversing the mat (Figure 9C).[118,130] Furthermore, it was found that the cells infiltrating the collagen mats showed pronounced development of microvilli, which is an indication of increased cell activity.[118]

The morphogenetic activity of polyP is reflected in the induction of the expression of specific genes involved in wound healing, as we could also show in animal experiments.[131] It should be noted that the beneficial effect of polyP on wound healing is supported by the antibacterial properties of the polymer, which not only acts as an inhibitor of matrix metalloproteinases and bacterial proteases that interfere with wound healing,[132] but also through the engulfment and from it resulting immobilization of bacteria by the formed polyP coacervate (see Figure 3A).

The ability of polyP coacervates to entrap cells or molecules can also be exploited in drug delivery. It has previously been shown that polyP nanoparticles can be loaded with certain drugs such as the bisphosphonate zoledronic acid, which is incorporated due to its chemical similarity to polyP. The resulting particles showed the properties of both components, the tumor growth-inhibiting effect of the bisphosphonate and the morphogenetic activity of polyP.[117]

In an elegant approach, we recently constructed core-shell particles consisting of a drug-loaded Ca-polyP nanoparticle core and a surrounding Ca-polyP coacervate shell loaded with a different, second drug.[133] A schematic presentation of the design of the polyP-based core-shell particles loaded with the two drugs is given in Figure 10A, which are prepared as follows. The amorphous Ca-polyP nanoparticles core is prepared under alkaline conditions (pH 10) from Na-polyP and $CaCl_2$ at a superstoichiometric Ca:P ratio of 2:1 in the presence of the first

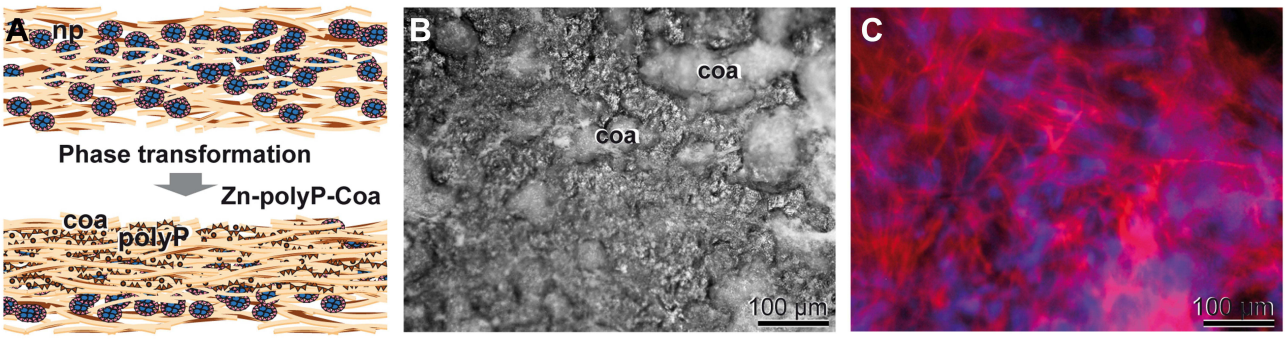

Figure 9 Activation of a compressed collagen wound mat supplemented with Zn-polyP nanoparticles by polyP coacervation upon contact with wound exudate during treatment of a patient suffering from a chronic wound. (**A**) Phase transformation of Zn-polyP nanoparticles (np) integrated in the mechanically compressed collagen wound mat into the coacervate (coa; schematic presentation). (**B** and **C**) Coacervate (coa) formation (**B**) and migration of cells (**C**) in the wound mat. A biopsy taken through the wound mat 3 weeks after the start of treatment shows that cells from the regenerating granulation tissue of the wound migrate into the mat. Cells were visualized by staining with rhodamine/phalloidin (actin; in red) and DRAQ5 (nuclei; in blue) (**C**). (**A**) Used with permission of Royal Society of Chemistry, from Müller WEG, Schepler H, Tolba E, et al. A physiologically active interpenetrating collagen network that supports growth and migration of epidermal keratinocytes: zinc-polyP nanoparticles integrated into compressed collagen. J Mater Chem B. 2020;8(27):5892–5902. © 2020; permission conveyed through Copyright Clearance Center, Inc.[118] (**B** and **C**) Adapted from Schepler H, Neufurth M, Wang SF, et al. Acceleration of chronic wound healing by bio-inorganic polyphosphate: in vitro studies and first clinical applications. Theranostics. 2022;12(1):18–34. © The Author(s). This is an open access article distributed under the terms of the Creative Commons Attribution License (https://creativecommons.org/licenses/by/4.0/).[130]

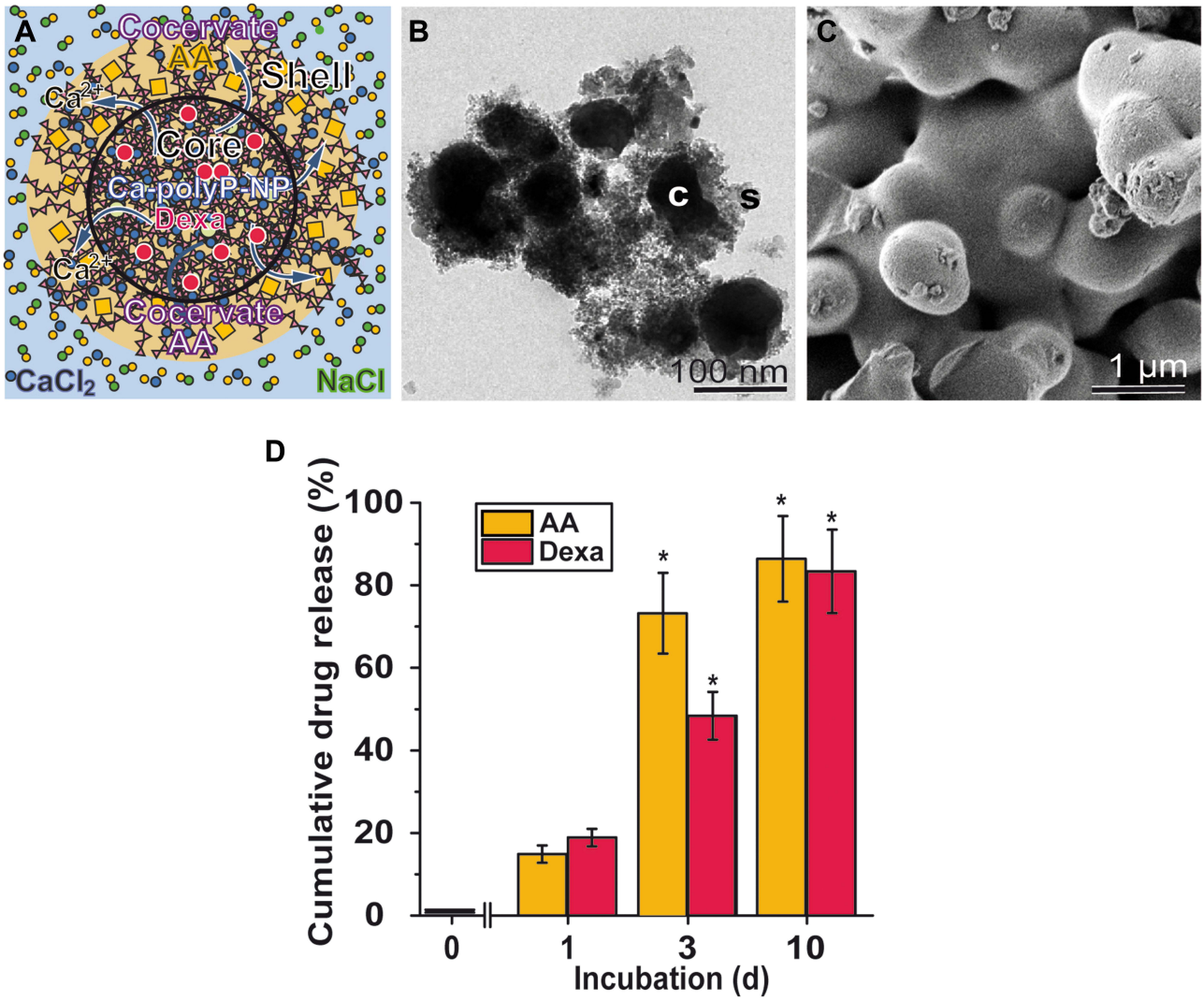

Figure 10 Drug delivery via core-shell particles consisting of a drug-1-loaded Ca-polyP nanoparticle core and a drug-2-loaded Ca-polyP coacervate shell. (**A**) Scheme of a polyP-based core-shell particle. The drug-loaded Ca-polyP nanoparticle core is prepared from Na-polyP and a stoichiometric excess of $CaCl_2$ at pH 10 in the presence of dexamethasone (Dexa; drug 1). Dexamethasone 21-phosphate is used, which binds via ionic interaction. The drug-loaded Ca-polyP-coacervate shell is prepared by exposure of the Ca-polyP nanoparticle core to a Na-polyP solution at pH 7. Coacervate formation is initiated by Ca^{2+} ions released from the nanoparticle core. L-ascorbate (AA; drug 2) used as a negatively charged second drug binds to the polyanionic polyP via Ca^{2+} bridges. (**B**) High-resolution TEM of the drug-loaded core-shell particles; c, core; s, shell. (**C**) SEM image of the core-shell particles. (**D**) Ascorbic acid and dexamethasone release kinetics from core-shell particles. The means ± SD of five independent experiments are shown (*$p < 0.005$). Adapted from Müller WEG, Tolba E, Wang SF, et al. Nanoparticle-directed and ionically forced polyphosphate coacervation: a versatile and reversible core-shell system for drug delivery. Sci Rep. 2020;10(1):17,147. © 2020 The Author(s). This article is licensed under a Creative Commons Attribution 4.0 International License (https://creativecommons.org/licenses/by/4.0/).[133]

drug, dexamethasone 21-phosphate, which is incorporated due to ionic interaction. In the next step, the coacervate shell is generated by exposure of the Ca-polyP core to a solution of soluble Na-polyP and ascorbic acid at pH 7. The coacervate is formed from the soluble polyP and Ca^{2+} ions that migrate from the nanoparticle core to the shell that is being formed. The second drug, L-ascorbate, is integrated in the outer shell by binding to polyP via Ca^{2+} bridge formation due to the negative charge of the molecule. The core-shell structure of the drug-loaded core-shell particles could be visualized by high-resolution TEM (Figure 10B). Their globular morphology analyzed by SEM is shown in Figure 10C.

In in vitro experiments, the core-shell particles showed not only the morphogenetic and energy-supplying activity of polyP, but also strong osteogenic activity, caused by the two incorporated active ingredients dexamethasone, which promotes osteogenic cell differentiation, and ascorbic acid, which induces collagen synthesis.[133] Studies on drug release kinetics revealed a fast process for the release of ascorbic acid and polyP from the coacervate shell, while the release of

the components of the nanoparticle core, dexamethasone and polyP, is slower, most likely since the latter process requires the transformation of the nanoparticles into the coacervate phase (Figure 10D).[133]

Polyphosphate and Morphogenetic Activity

Morphogenetic activity, as described above, is a characteristic property of polyP, which the polymer shows only after transformation of polyP nanoparticles into the coacervate phase. In its specific formulation, polyP can even determine the direction of cell differentiation. The identification of molecules capable of controlling the direction of stem cell differentiation by inducing specific gene expression is a major challenge and of great importance in tissue engineering and repair. PolyP actually represents such a molecule. The direction of differentiation is determined by the counterion of the polymer.[134] It was found that polyP can induce the differentiation of MSC into either the osteogenic, chondrogenic, myogenic, or tenogenic lineage, depending on the counterion.

The mechanism by which polyP stimulates cell growth and differentiation involves specific signaling pathways such as the mTOR/Wnt/β-catenin[135] or FGF (fibroblast growth factor) signaling pathway,[136,137] as well as the expression of specific transcription factors such as RUNX2 (Runt-related transcription factor 2) and SOX9 (SRY-box transcription factor 9).[50,122,123,138] Activation of the protein kinase mTOR (mammalian target of rapamycin) by polyP leads to phosphorylation of PHAS-I, a protein that binds to the eukaryotic initiation factor eIF-4E and is involved in regulation of protein synthesis and cell proliferation.[139] Ca-polyP nanoparticles and Sr-polyP nanoparticles induce the expression of genes that lead to the differentiation of MSC into mineralizing osteoblasts,[52] while Mg-polyP nanoparticles promote the differentiation into chondrocytes.[50] Specific genes expressed in the presence of amorphous Ca-polyP nanoparticles include RUNX2 (differentiation of MSC into osteoblasts),[138] ALP[140] and bone morphogenetic protein 2 (BMP-2).[140] The amorphous Sr-polyP nanoparticles induce the expression of sclerostin, an inhibitor of canonical Wnt/β-catenin signaling,[52] while Mg-polyP nanoparticles promote the expression of SOX9 (differentiation of MSC into chondrocytes) and ALP, as well as the collagen types 2A1 and 3A1 and aggrecan.[50,123] Accordingly, depending on the counterion, these polyP nanoparticles can be used to regenerate and repair bone or cartilage tissue.[52,53,121] At present, there is little knowledge as to which cell surface receptors polyP binds to, or whether polyP primarily interferes with receptor ligand interactions. PolyP has been shown to bind to purinergic receptors ($P2Y_1$), resulting in activation of phospholipase C and an increase in intracellular-free calcium in astrocytes.[141] Results obtained in the unicellular eukaryote *Dictyostelium discoideum* indicate that other G protein-coupled receptors may also be involved in the response of mammalian cells to extracellular polyP.[142] It should be noted that polyP can also be taken up by cells, most likely via a clathrin-mediated mechanism,[112,143] and also interact with intracellular proteins.

Polyphosphate and Energy Generation

The second characteristic of polyP that requires formation of the coacervate phase from the nanoparticulate storage form of the polymer, the supply of metabolic energy, makes this polymer unique for tissue regeneration applications. Tissue regeneration and repair requires a lot of energy, an aspect that has received little attention in the design of scaffold materials in regenerative medicine. Scaffold materials based on organic molecules that modulate the metabolic energy state of cells have only been developed to a limited extent.[144] However, with polyP, we have an inorganic molecule that is attracting increasing interest as a source of metabolic energy. PolyP can store many times the energy present in ATP in the form of energy-rich phosphate residues linked via high-energy anhydride bonds, each of which can release an energy of –30.5 $kJ \cdot mol^{-1}$ after hydrolytic bond cleavage. This energy is required not only for processes within cells, but also for processes in the extracellular space, including the organization and function of the ECM structure. Extracellular ATP concentrations are much lower than cytosolic ATP levels, ranging only from 1 to 100 nM compared to 1 to 10 mM of intracellular ATP.[145] Extracellular ATP-consuming reactions or other nucleotide-dependent processes involve not only the phosphorylation of ECM proteins by extracellular kinases,[146] but also the function of extracellular chaperones such as clusterin.[147,148]

In bacteria, polyP can act as a source for ATP production via the reversible reaction of polyP kinase. A related enzyme has not been found in mammalian or human cells and tissues. Hydrolytic degradation by the ubiquitous ALP, which is present both intra- and extracellularly, only leads to dissipation of the energy stored in the polyP phosphoanhydride bonds in the form of heat, which

cannot be converted back into chemical energy. Inhibitor experiments, however, provided evidence that polyP acts as a donor for metabolically usable energy, of ATP, through the interaction of ALP with a second enzyme, ADK, which is also bound to the outer cell membrane.[81,127] Experiments with SaOS-2 revealed that addition of polyP to these cells leads to a strong increase of ATP in the culture medium.[127] This rise in the ATP level could be prevented by administrating levamisole, an inhibitor of ALP activity. Evidence that ADK is involved as the second enzyme came from results with P^1,P^5-di(adenosine-5′) pentaphosphate (Ap_5A), an ADK inhibitor, which led to a drop of the ratio between the extracellular levels of ATP and ADP.[81] From this, it was concluded that the formation of ATP from polyP requires the combined action of the two enzymes ALP and ADK, which act as an enzyme pair.

From these results, it has been suggested that ATP formation from polyP comprises two steps; firstly, a phosphotransfer reaction from polyP to AMP forming ADP, which secondly undergoes ADK-catalyzed interconversion to ATP and AMP consuming a second ADP molecule.[3] In this way, one ATP molecule can be produced from each energy-rich phosphate in the polyP chain. In reality, the yield is likely lower since the phosphotransfer reaction competes with the hydrolytic cleavage of the phosphoanhydride bond and depends on the availability of AMP. The second ADP molecule required for the ADK reaction is generated from the end product of the ALP/ADK-reaction, from ATP, by subsequent kinase or ATPase reactions. Due to their exothermic nature, the latter reactions are expected to shift the chemical equilibrium of ALP and ADK towards ATP formation.

Both ALP and ADK are associated with the plasma membrane and also occur extracellularly. In the proposed mechanism of the ALP-mediated phosphotransfer reaction, enzymatic cleavage of the terminal phosphate group of polyP generates a metaphosphate species, which is bound to the catalytic site of the enzyme prior to transfer to AMP, leading to ADP formation.[3]

During the catalytic cycle, the two monomeric subunits of the ALP homodimer, attached to the cell membrane via a GPI anchor, alternately undergo conformational changes involved in the catalytic mechanism of the enzyme. The catalytic site of each ALP monomer contains one Mg^{2+} ion in addition to the two Zn^{2+} ions associated with the metaphosphate intermediate.[3,75,77] The Mg^{2+} ion is involved in the allosteric activation of the enzyme. Depending on Mg^{2+}, the affinity of the ALP subunit for polyP is high (Mg^{2+} is present) or low (absence of Mg^{2+}).[3] In the course of the reaction, both subunits switch from the low-affinity state to the high-affinity state and back in a mutually controlled manner, which leads to a gradual degradation of the polyP chain with participation of both subunits.[3]

Future Directions

The development of specifically designed coacervates opens a variety of potential biomedical applications.[149] Coacervate formation in general, including phase separation of polyP solutions, can be controlled by a series of environmental stimuli such as pH, temperature, ionic strength or specific electrolytes.[31–33,150] This property of the polyP coacervates allows the development of novel stimuli-responsive systems for biomedical or technological applications.

In this regard, polyP, either exogenously administered or endogenously produced and delivered by platelets, can be considered as a bio-intelligent material. As described in this article, the physiological activity of this biomolecule depends on the phase of the polymer, which can exist either in a stable but inactive form as particulate polyP nanoparticle or in a physiologically active phase as a polyP coacervate with morphogenetic activity and the ability to deliver metabolic energy in cooperation with the ALP/ADK pair. The specific state of polyP (nanoparticles or coacervate) depends on various parameters such as the pH and the availability and type of divalent cations (Ca^{2+}, Mg^{2+}, Zn^{2+} and others) in the surrounding milieu, as well as protein concentration, and could be modulated by changes in the external conditions that are either physiologically or pathologically. For example, bacterial infections occurring during wound healing can cause the pH value of the wound bed, which is optimal in the slightly acidic range, to rise to more alkaline values[151] and ALP activity to increase.[152] The activity of extracellular ALP also increases during the progression of the granulation phase of wound healing.[153] In addition, it has been reported that Zn^{2+} ions accumulate during wound healing.[154] Therefore, it is assumed that polyP can change reversibly, eg, during wound healing, depending on the stimulus, between the amorphous nanoparticulate state and the morphogenetically active, energy-delivering coacervate phase. By coupling with a decision-making system and an effector, polyP as a sensor together with the ALP/ADK system could even be part of a bio-artificial intelligence system.[155,156] Future studies need to demonstrate the potential existence

of such circuits with polyP that triggers and modulates the specific response of cells and tissues to internal or external stimuli. First successes in this direction have already been achieved through the development of advanced implant materials and drug delivery systems capable of forming in situ polyP nanoparticles,[124] which are converted into the physiologically active coacervate by protein at the injured tissue site.[118,130]

There is an increasing interest in such multifunctional, advanced hydrogel materials, not only for biomedical but also technical applications.[157] Such materials are not only needed for applications in bone and cartilage tissue engineering or wound healing, as described in this article, but also in a variety of other applications, such as biologization of inert surfaces, as dental sealants,[158] or even as a prophylactic or therapeutic agent against infection by SARS-CoV-2 virus[159] due to the antiviral activity of the polymer.[160–162] For example, a polyP-containing formulation has been developed which, when applied as an aerosol, can entrap the virus particles after virus/mucus contact and also block the virus-receptor interaction.[163] Future applications of polyP-containing hydrogels could also include a potential application in photothermal tumor therapy. For example, it has recently been shown that chitosan-based hydrogels can be endowed with photothermal conversion capability by incorporation of infrared light absorbing polyaniline, allowing the development of a non-invasive method for in situ tumor killing by hyperthermia.[164]

Future applications of polyP-containing hydrogels could also take advantage of the polymer's still untapped ability in tissue engineering to modulate reactive oxygen species (ROS)-based systems, either through the generation of catalytically active manganese phosphate ($MnHPO_4$), which exhibits superoxide dismutase (SOD)-like activity (dismutation of superoxide radicals [$O_2^{\cdot -}$] to hydrogen peroxide [H_2O_2] and oxygen)[165] via ALP-mediated degradation of Mn-polyP, or by inhibition of hydroxyl radicals [·OH] production via chelation and stabilization of Fe^{3+} ions used to regenerate Fe^{2+} in Fenton reaction.[166,167] A first hydrogel containing an integrated Fe^{2+}/Fe^{3+} cyclic redox system based on a MoS_2/alginate/Fe hydrogel catalyst, which enables an infrared radiation controlled ·OH generation via the Fenton reaction, has recently been realized.[168] The importance of polyP, particularly in the regulation of the mitochondrial oxidative stress response has been demonstrated in experiments using mitochondrial polyP depleted mammalian cells.[169] Depletion of mitochondrial polyP was found to cause increased mitochondrial ROS production, most likely due a dysregulation of redox homeostasis, resulting in a reduced rate of oxidative phosphorylation and a shift towards the pentose phosphate and glycolysis pathways.[170,171]

Conclusions

Coacervation has been recognized as an important physiological process both intra- and extracellularly. In contrast to the formation of complex coacervates, little was hitherto known about the formation of simple coacervates. The most prominent example, as described here, are coacervates, which are formed from the polyanion polyP and certain (usually divalent) counter-cations. While various models and mechanisms for complex coacervate formation have been proposed, the formation of simple polyP coacervates has remained a mystery and only scarcely investigated. Recent results on coacervate formation of polyP in the presence of metal cations are summarized and discussed in this review, which shed some light on this process, which is important to understand, especially as polyP has been shown to be a unique—the only—inorganic polymer that is both morphogenetically active and capable of providing metabolic energy, particularly for regenerative medical applications. Furthermore, polyP coacervation has been shown to be a mechanism for entrapping and inactivating bacterial and viral pathogens. Investigations into the kinetics of polyP coacervations revealed that this process can be divided into distinct phases, some of which are different but also have some similarities to the formation of complex coacervates. Indeed, it can be assumed that the polyP counterions involved in coacervation, such as Ca^{2+} ions, form a polymer-like assembly that acts in a manner similar to a polycation in complex polyP coacervation.

Also of particular interest is the ability of the polymer to exist in both a coacervate phase and a nanoparticle phase alongside the soluble form of the polymer, due to the different properties of both polyP phases. While polyP nanoparticles represent a rather biologically inert storage form of the polymer that resists attack by polyP-degrading enzymes such as ALP over long periods of time, the coacervate is the biologically active form that stimulates cell growth and differentiation and acts as a source of ATP that is required for cell and tissue function. Insight into polyP coacervate formation also allows for a better understanding of polyP nanoparticle formation and the interconversion of both polyP phases.

Acknowledgments

W.E.G.M. is a holder of an ERC Advanced Investigator Grant (No. 268476). In addition, W.E.G.M. obtained three ERC-PoC grants (Si-Bone-PoC, Grant No. 324564; MorphoVES-PoC, Grant No. 662486; and ArthroDUR, Grant No. 767234). We also acknowledge funding from the European Commission (grants BIO-SCAFFOLDS No. 604036 and BlueGenics No. 311848). Finally, this work was supported by grants from the Deutsche Forschungsgemeinschaft – Priority Programme 1420 (Schr 277/10-3), the Federal Ministry of Education and Research (BMBF - SKIN-ENERGY - FKZ 13GW0403B), the Federal Ministry for Economic Affairs and Energy (ZIM - ZF4294001 CS6) and the BiomaTiCS research initiative of the University Medical Center, Mainz.

Author Contributions

All authors made a significant contribution to the work reported, have drafted or written, or substantially revised or critically reviewed the article, have agreed on the journal to which the article is submitted, reviewed and agreed on the article before submission, and agreed to take responsibility and be accountable for the contents of the article.

Disclosure

The authors report no conflicts of interest in this work.

References

1. Kornberg A, Rao NN, Ault-Riché D. Inorganic polyphosphate: a molecule of many functions. *Annu Rev Biochem*. 1999;68(1):89–125. doi:10.1146/annurev.biochem.68.1.89
2. Kulaev IS, Vagabov VM, Kulakovskaya TV. *The Biochemistry of Inorganic Polyphosphates*. Chichester: John Wiley & Sons; 2004.
3. Müller WEG, Schröder HC, Wang XH. Inorganic polyphosphates as storage for and generator of metabolic energy in the extracellular matrix. *Chem Rev*. 2019;119(24):12337–12374. doi:10.1021/acs.chemrev.9b00460
4. Corbridge DEC. *Phosphorus: Chemistry, Biochemistry and Technology*. 6th ed. Boca Raton: CRC Press, Taylor & Francis Group; 2013.
5. Müller WEG, Wang SF, Tolba E, et al. Transformation of amorphous polyphosphate nanoparticles into coacervate complexes: an approach for the encapsulation of mesenchymal stem cells. *Small*. 2018;14(27):e1801170. doi:10.1002/smll.201801170
6. Nakashima KK, Vibhute MA, Spruijt E. Biomolecular chemistry in liquid phase separated compartments. *Front Mol Biosci*. 2019;6:21. doi:10.3389/fmolb.2019.00021
7. Spruijt E, Westphal AH, Borst JW, Cohen Stuart MA, van der Gucht J. Binodal compositions of polyelectrolyte complexes. *Macromolecules*. 2010;43(15):6476–6484. doi:10.1021/ma101031t
8. Astoricchio E, Alfano C, Rajendran L, Temussi PA, Pastore A. The wide world of coacervates: from the sea to neurodegeneration. *Trends Biochem Sci*. 2020;45(8):706–717. doi:10.1016/j.tibs.2020.04.006
9. De Kruif CG, Weinbreck F, de Vries R. Complex coacervation of proteins and anionic polysaccharides. *Curr Opin Colloid Interface Sci*. 2004;9(5):340–349. doi:10.1016/j.cocis.2004.09.006
10. Feric M, Vaidya N, Harmon TS, et al. Coexisting liquid phases underlie nucleolar subcompartments. *Cell*. 2016;165(7):1686–1697. doi:10.1016/j.cell.2016.04.047
11. Murray DT, Kato M, Lin Y, et al. Structure of FUS protein fibrils and its relevance to self-assembly and phase separation of low-complexity domains. *Cell*. 2017;171(3):615–627.e16. doi:10.1016/j.cell.2017.08.048
12. Van der Gucht J, Spruijt E, Lemmers M, Cohen Stuart MA. Polyelectrolyte complexes: bulk phases and colloidal systems. *J Colloid Interface Sci*. 2011;361(2):407–422. doi:10.1016/j.jcis.2011.05.080
13. Gomes E, Shorter J. The molecular language of membraneless organelles. *J Biol Chem*. 2019;294(18):7115–7127. doi:10.1074/jbc.TM118.001192
14. Deng NN. Complex coacervates as artificial membraneless organelles and protocells. *Biomicrofluidics*. 2020;14(5):051301. doi:10.1063/5.0023678
15. Wang B, Zhang L, Dai T, et al. Liquid-liquid phase separation in human health and diseases. *Signal Transduct Target Ther*. 2021;6(1):290. doi:10.1038/s41392-021-00678-1
16. Yewdall NA, André AAM, Lu T, Spruijt E. Coacervates as models of membrane-less organelles. *Curr Opin Colloid Interface Sci*. 2021;52:101416. doi:10.1016/j.cocis.2020.101416
17. Oparin AI, Yevreinova TN, Larionova TI, Davydova IM. Synthesis and disintegration of starch in coacervate drops. *Dokl Akad Nauk SSSR*. 1962;143:980–983.
18. Van Haren MHI, Nakashima KK, Spruijt E. Coacervate-based protocells: integration of life-like properties in a droplet. *J Syst Chem*. 2020;8:107–120.
19. Abbas M, Lipiński WP, Wang J, Spruijt E. Peptide-based coacervates as biomimetic protocells. *Chem Soc Rev*. 2021;50(6):3690–3705. doi:10.1039/d0cs00307g
20. Blocher WC, Perry SL. Complex coacervate-based materials for biomedicine. *Wiley Interdiscip Rev Nanomed Nanobiotechnol*. 2017;9(4). doi:10.1002/wnan.1442
21. Stewart RJ, Wang CS, Shao H. Complex coacervates as a foundation for synthetic underwater adhesives. *Adv Colloid Interface Sci*. 2011;167(1–2):85–93. doi:10.1016/j.cis.2010.10.009

22. Kaur S, Weerasekare GM, Stewart RJ. Multiphase adhesive coacervates inspired by the sandcastle worm. *ACS Appl Mater Interfaces*. 2011;3(4):941–944. doi:10.1021/am200082v
23. Zhao Q, Lee DW, Ahn BK, et al. Underwater contact adhesion and microarchitecture in polyelectrolyte complexes actuated by solvent exchange. *Nat Mater*. 2016;15(4):407–412. doi:10.1038/nmat4539
24. Sing CE, Perry SL. Recent progress in the science of complex coacervation. *Soft Matter*. 2020;16(12):2885–2914. doi:10.1039/d0sm00001a
25. Rumyantsev AM, Jackson NE, de Pablo JJ. Polyelectrolyte complex coacervates: recent developments and new frontiers. *Annu Rev Condens Matter Phys*. 2021;12(1):155–176. doi:10.1146/annurev-conmatphys-042020-113457
26. Bungenberg de Jong HG, Kruyt HR. Crystallisation, coacervation, flocculation. In: Kruyt HR, editor. *Colloid Science*. Vol. 2. Amsterdam: Elsevier; 1949:232–258.
27. Priftis D, Laugel N, Tirrell M. Thermodynamic characterization of polypeptide complex coacervation. *Langmuir*. 2012;28(45):15947–15957. doi:10.1021/la302729r
28. Fu J, Schlenoff JB. Driving forces for oppositely charged polyion association in aqueous solutions: enthalpic, entropic, but not electrostatic. *J Am Chem Soc*. 2016;138(3):980–990. doi:10.1021/jacs.5b11878
29. Liu Y, Winter HH, Perry SL. Linear viscoelasticity of complex coacervates. *Adv Colloid Interface Sci*. 2017;239:46–60. doi:10.1016/j.cis.2016.08.010
30. Donau C, Späth F, Sosson M, et al. Active coacervate droplets as a model for membraneless organelles and protocells. *Nat Commun*. 2020;11(1):5167. doi:10.1038/s41467-020-18815-9
31. Love C, Steinkühler J, Gonzales DT, et al. Reversible pH-responsive coacervate formation in lipid vesicles activates dormant enzymatic reactions. *Angew Chem Int Ed Engl*. 2020;59(15):5950–5957. doi:10.1002/anie.201914893
32. Martin N, Tian L, Spencer D, Coutable-Pennarun A, Anderson JLR, Mann S. Photoswitchable phase separation and oligonucleotide trafficking in DNA coacervate microdroplets. *Angew Chem Int Ed Engl*. 2019;58(41):14594–14598. doi:10.1002/anie.201909228
33. Deng NN, Huck WTS. Microfluidic formation of monodisperse coacervate organelles in liposomes. *Angew Chem Int Ed Engl*. 2017;56(33):9736–9740. doi:10.1002/anie.201703145
34. Danielsen SPO, Panyukov S, Rubinstein M. Ion pairing and the structure of gel coacervates. *Macromolecules*. 2020;53(21):9420–9442. doi:10.1021/acs.macromol.0c01360
35. Brangwynne CP, Tompa P, Pappu RV. Polymer physics of intracellular phase transitions. *Nat Phys*. 2015;11(11):899–904. doi:10.1038/nphys3532
36. Chang LW, Lytle TK, Radhakrishna M, et al. Sequence and entropy-based control of complex coacervates. *Nat Commun*. 2017;8(1):1273. doi:10.1038/s41467-017-01249-1
37. Delaney KT, Fredrickson GH. Theory of polyelectrolyte complexation-complex coacervates are self-coacervates. *J Chem Phys*. 2017;146(22):224902. doi:10.1063/1.4985568
38. Nakashima KK, André AAM, Spruijt E. Enzymatic control over coacervation. *Methods Enzymol*. 2021;646:353–389. doi:10.1016/bs.mie.2020.06.007
39. Gupta A, Bohidar HB. Kinetics of phase separation in systems exhibiting simple coacervation. *Phys Rev E Stat Nonlin Soft Matter Phys*. 2005;72(1 Pt 1):011507. doi:10.1103/PhysRevE.72.011507
40. Masson NC, de Souza EF, Galembeck F. Calcium and iron(III) polyphosphate gel formation and aging. *Colloids Surfaces A: Physicochem Eng Aspects*. 1997;121(2–3):247–255. doi:10.1016/S0927-7757(96)03985-4
41. Becker P. Phosphoric acid and phosphates. In: *Kirk-Othmer Encyclopedia of Chemical Technology*. 4th ed. New York: John Wiley & Sons; Vol. 18, 1991:669–718.
42. Glonek T. Did cyclic metaphosphates have a role in the origin of life? *Orig Life Evol Biosph*. 2021;51(1):1–60. doi:10.1007/s11084-021-09604-5
43. Rashchi F, Finch JA. Polyphosphates: a review. Their chemistry and application with particular reference to mineral processing. *Miner Eng*. 2000;13(10−11):1019–1035. doi:10.1016/S0892-6875(00)00087-X
44. Majling J, Hanic F. Phase chemistry of condensed phosphates. In: Grayson M, Griffith EJ, editors. *Topics in Phosphorus Chemistry*. Vol. 10. New York: Wiley; 1980:341–502.
45. Katchman BJ, Smith HE. Diffusion of synthetic and natural polyphosphates. *Arch Biochem Biophys*. 1958;75(2):396–402. doi:10.1016/0003-9861(58)90438-7
46. Van Wazer JR, ed. *Phosphorus and Its Compounds: Chemistry*. New York: Interscience Publishers; Vol. 1, 1958.
47. Do Rego Monteiro VA, de Souza EF, de Azevedo MM, Galembeck F. Aluminum polyphosphate nanoparticles: preparation, particle size determination, and microchemistry. *J Colloid Interface Sci*. 1999;217(2):237–248. doi:10.1006/jcis.1999.6381
48. Rao NN, Gómez-García MR, Kornberg A. Inorganic polyphosphate: essential for growth and survival. *Annu Rev Biochem*. 2009;78:605–647. doi:10.1146/annurev.biochem.77.083007.093039
49. Müller WEG, Tolba E, Schröder HC, et al. A new polyphosphate calcium material with morphogenetic activity. *Mater Lett*. 2015;148:163–166. doi:10.1016/j.matlet.2015.02.070
50. Müller WEG, Ackermann M, Tolba E, et al. A bio-imitating approach to fabricate an artificial matrix for cartilage tissue engineering using magnesium-polyphosphate and hyaluronic acid. *RSC Adv*. 2016;6(91):88559–88570. doi:10.1039/C6RA17043A
51. Wang XH, Huang J, Wang K, et al. The morphogenetically active polymer, inorganic polyphosphate complexed with $GdCl_3$, as an inducer of hydroxyapatite formation *in vitro*. *Biochem Pharmacol*. 2016;102:97–106. doi:10.1016/j.bcp.2015.12.011
52. Müller WEG, Tolba E, Ackermann M, et al. Fabrication of amorphous strontium polyphosphate microparticles that induce mineralization of bone cells in vitro and in vivo. *Acta Biomater*. 2017;50:89–101. doi:10.1016/j.actbio.2016.12.045
53. Wang XH, Schröder HC, Müller WEG. Amorphous polyphosphate, a smart bioinspired nano-/bio-material for bone and cartilage regeneration: towards a new paradigm in tissue engineering. *J Mater Chem B*. 2018;6(16):2385–2412. doi:10.1039/c8tb00241j
54. Galembeck A. Aluminum polyphosphate gels structural evolution probed by NMR spectroscopy. *J Braz Chem Soc*. 2003;14(6):930–935. doi:10.1590/S0103-50532003000600010
55. Matheja J, Degens ET. *Structural Molecular Biology of Phosphates*. Stuttgart: Gustav Fischer Verlag; 1971:78–90.

56. Thilo E, Wicker W. Zur Chemie der kondensierten Phosphate und Arsenate. XVIII. Anionenhydrolyse der kondensierten Phosphate in verdünnter wässriger Lösung [On the chemistry of condensed phosphates and arsenates. XVIII. Anion hydrolysis of the condensed phosphates in dilute aqueous solution]. *Z Anorg Allg Chem*. 1957;Vol. 291:164–185. doi:10.1002/zaac.19572910120
57. Davis BD. On the importance of being ionized. *Arch Biochem Biophys*. 1958;78(2):497–509. doi:10.1016/0003-9861(58)90374-6
58. Westheimer FH. Why nature chose phosphates. *Science*. 1987;235(4793):1173–1178. doi:10.1126/science.2434996
59. De Jager HJ, Heyns AM. Kinetics of acid-catalyzed hydrolysis of a polyphosphate in water. *J Phys Chem A*. 1998;102(17):2838–2841. doi:10.1021/jp9730252
60. De Jager H, Heyns AM. Study of the hydrolysis of sodium polyphosphate in water using Raman spectroscopy. *Appl Spectrosc*. 1998;52 (6):808–814. doi:10.1366/0003702981944535
61. Morrissey JH, Choi SH, Smith SA. Polyphosphate: an ancient molecule that links platelets, coagulation, and inflammation. *Blood*. 2012;119 (25):5972–5979. doi:10.1182/blood-2012-03-306605
62. Verhoef JJ, Barendrecht AD, Nickel KF, et al. Polyphosphate nanoparticles on the platelet surface trigger contact system activation. *Blood*. 2017;129(12):1707–1717. doi:10.1182/blood-2016-08-734988
63. Schröder HC, Müller WEG, eds. *Inorganic Polyphosphates: Biochemistry, Biology, Biotechnology.* Berlin/Heidelberg: Springer (Prog Mol Subcell Biol. 23); 1999.
64. Ruiz FA, Lea CR, Oldfield E, Docampo R. Human platelet dense granules contain polyphosphate and are similar to acidocalcisomes of bacteria and unicellular eukaryotes. *J Biol Chem*. 2004;279(43):44250–44257. doi:10.1074/jbc.M406261200
65. Leyhausen G, Lorenz B, Zhu H, et al. Inorganic polyphosphate in human osteoblast-like cells. *J Bone Miner Res*. 1998;13(5):803–812. doi:10.1359/jbmr.1998.13.5.803
66. Schröder HC, Kurz L, Müller WEG, Lorenz B. Polyphosphate in bone. *Biochemistry*. 2000;65(3):296–303. PMID: 10739471.
67. Omelon S, Georgiou J, Henneman ZJ, et al. Control of vertebrate skeletal mineralization by polyphosphates. *PLoS One*. 2009;4(5):e5634. doi:10.1371/journal.pone.0005634
68. Bowlin MQ, Gray MJ. Inorganic polyphosphate in host and microbe biology. *Trends Microbiol*. 2021;29(11):1013–1023. doi:10.1016/j.tim.2021.02.002
69. Pavlov E, Aschar-Sobbi R, Campanella M, Turner RJ, Gómez-García MR, Abramov AY. Inorganic polyphosphate and energy metabolism in mammalian cells. *J Biol Chem*. 2010;285(13):9420–9428. doi:10.1074/jbc.M109.013011
70. Angelova PR, Baev AY, Berezhnov AV, Abramov AY. Role of inorganic polyphosphate in mammalian cells: from signal transduction and mitochondrial metabolism to cell death. *Biochem Soc Trans*. 2016;44(1):40–45. doi:10.1042/BST20150223
71. Hothorn M, Neumann H, Lenherr ED, et al. Catalytic core of a membrane-associated eukaryotic polyphosphate polymerase. *Science*. 2009;324 (5926):513–516. doi:10.1126/science.1168120
72. Docampo R, de Souza W, Miranda K, Rohloff P, Moreno SN. Acidocalcisomes − conserved from bacteria to man. *Nat Rev Microbiol*. 2005;3 (3):251–261. doi:10.1038/nrmicro1097
73. Abramov AY, Fraley C, Diao CT, et al. Targeted polyphosphatase expression alters mitochondrial metabolism and inhibits calcium-dependent cell death. *Proc Natl Acad Sci U S A*. 2007;104(46):18091–18096. doi:10.1073/pnas.0708959104
74. Ahn K, Kornberg A. Polyphosphate kinase from *Escherichia coli*. Purification and demonstration of a phosphoenzyme intermediate. *J Biol Chem*. 1990;265(20):11734–11739. doi:10.1016/S0021-9258(19)38459-5
75. Millán JL. Alkaline phosphatases: structure, substrate specificity and functional relatedness to other members of a large superfamily of enzymes. *Purinergic Signal*. 2006;2(2):335–341. doi:10.1007/s11302-005-5435-6
76. Lorenz B, Schröder HC. Mammalian intestinal alkaline phosphatase acts as highly active exopolyphosphatase. *Biochim Biophys Acta*. 2001;1547(2):254–261. doi:10.1016/S0167-4838(01)00193-5
77. Hoylaerts MF, Manes T, Millán JL. Mammalian alkaline phosphatases are allosteric enzymes. *J Biol Chem*. 1997;272(36):22781–22787. doi:10.1074/jbc.272.36.22781
78. Halling Linder C, Englund UH, Narisawa S, Millán JL, Magnusson P. Isozyme profile and tissue-origin of alkaline phosphatases in mouse serum. *Bone*. 2013;53(2):399–408. doi:10.1016/j.bone.2012.12.048
79. Duarte F, Amrein BA, Kamerlin SC. Modeling catalytic promiscuity in the alkaline phosphatase superfamily. *Phys Chem Chem Phys*. 2013;15 (27):11160–11177. doi:10.1039/c3cp51179k
80. Pabis A, Kamerlin SC. Promiscuity and electrostatic flexibility in the alkaline phosphatase superfamily. *Curr Opin Struct Biol*. 2016;37:14–21. doi:10.1016/j.sbi.2015.11.008
81. Müller WEG, Wang SF, Neufurth M, et al. Polyphosphate as a donor of high-energy phosphate for the synthesis of ADP and ATP. *J Cell Sci*. 2017;130(16):2747–2756. doi:10.1242/jcs.204941
82. Tammenkoski M, Koivula K, Cusanelli E, et al. Human metastasis regulator protein H-prune is a short-chain exopolyphosphatase. *Biochemistry*. 2008;47(36):9707–9713. doi:10.1021/bi8010847
83. Harada K, Itoh H, Kawazoe Y, et al. Polyphosphate-mediated inhibition of tartrate-resistant acid phosphatase and suppression of bone resorption of osteoclasts. *PLoS One*. 2013;8(11):e78612. doi:10.1371/journal.pone.0078612
84. Kumble KD, Kornberg A. Endopolyphosphatases for long chain inorganic polyphosphate in yeast and mammals. *J Biol Chem*. 1996;271 (43):27146–27151. doi:10.1074/jbc.271.43.27146
85. Umegaki T, Nakayama Y, Kanazawa T. Thermal change of magnesium high polyphosphate coacervates. *Bull Chem Soc Jpn*. 1976;49 (8):2105–2107. doi:10.1246/bcsj.49.2105
86. Gomez F, Vast P, Barbieux F, Llewellyn P, Rouquerol F. Controlled transformation rate thermal analysis: an inverse method allowing the characterisation of the thermal behaviour of polyphosphate glasses. *High Temp High Press*. 1998;30:575–580. doi:10.1068/HTEC359
87. Silva MA, Franco DF, de Oliveira LF. New insight on the structural trends of polyphosphate coacervation processes. *J Phys Chem A*. 2008;112 (24):5385–5389. doi:10.1021/jp801585v
88. Franco DF, Barud HS, Santagneli S, et al. Preparation and structural characterization of sodium polyphosphate coacervate as a precursor for optical materials. *Mater Chem Phys*. 2016;180:114–121. doi:10.1016/j.matchemphys.2016.05.049
89. Lima ECO, Galembeck F. Thermoreversible gel formation from aqueous aluminum polyphosphate solutions. *J Colloid Interface Sci*. 1994;166:309–315. doi:10.1006/JCIS.1994.1300

90. Palavit G, Montagne L, Delaval R. Preparation of zinc-phosphate glass precursors by coacervation. *J Non Cryst Solids*. 1995;189(3):277–282. doi:10.1016/0022-3093(95)00236-7
91. Willot G, Gomez F, Vasa P, et al. Preparation of zinc sodium polyphosphates glasses from coacervates precursors. Characterisation of the obtained glasses, and their applications. *C R Chimie*. 2002;5:899–906. doi:10.1016/S1631-0748(02)01454-6
92. Dias Filho FA, Carlos LD, Messadeq Y, Ribeiro SJ. Spectroscopic study and local coordination of polyphosphate colloidal systems. *Langmuir*. 2005;21(5):1776–1783. doi:10.1021/la0476837
93. De Oliveira LFC, Silva MAP, Brandão AR, et al. Amorphous manganese polyphosphates: preparation, characterization and incorporation of azo dyes. *J Solgel Sci Technol*. 2009;50(2):158–163. doi:10.1007/s10971-009-1965-7
94. Kopp W, Barud HS, Paz MF, Bueno LA, Giordano RLC, Ribeiro SJL. Calcium polyphosphate coacervates: effects of thermal treatment. *J Solgel Sci Technol*. 2012;63:219–223. doi:10.1007/s10971-012-2749-z
95. Momeni A, Filiaggi MJ. Comprehensive study of the chelation and coacervation of alkaline earth metals in the presence of sodium polyphosphate solution. *Langmuir*. 2014;30(18):5256–5266. doi:10.1021/la500474j
96. Momeni A, Filiaggi MJ. Degradation and hemostatic properties of polyphosphate coacervates. *Acta Biomater*. 2016;41:328–341. doi:10.1016/j.actbio.2016.06.002
97. Franco DF, Manzani D, Barud HS, et al. Structural investigation of nickel polyphosphate coacervate glass–ceramics. *RSC Adv*. 2016;6:91150–91156. doi:10.1039/C6RA20696D
98. Franco DF, De Oliveira Barud HG, Barud HS, et al. A review on polyphosphate coacervates – structural properties and bioapplications. *J Solgel Sci Technol*. 2020;94:531–543. doi:10.1007/s10971-020-05228-9
99. Bungenberg de Jong HG, Kruyt HR. Koazervation (Entmischung in kolloiden systemen) [Coacervation (segregation in colloidal systems)]. *Koll Z*. 1930;50:39–48. doi:10.1007/BF01422833
100. Cini N, Ball V. Polyphosphates as inorganic polyelectrolytes interacting with oppositely charged ions, polymers and deposited on surfaces: fundamentals and applications. *Adv Colloid Interface Sci*. 2014;209:84–97. doi:10.1016/j.cis.2014.01.011
101. Sabbagh I, Delsanti M. Solubility of highly charged anionic polyelectrolytes in presence of multivalent cations: specific interaction effect. *Eur Phys J E*. 2000;1(1):75–86. doi:10.1007/s101890050009
102. Sugano T, Kubo K. Enthalpy and entropy of complex formation of polyphosphate ions with alkaline-earth metal ions. *Nippon Kagaku Kaishi*. 1977;1977(4):500–503. doi:10.1246/nikkashi.1977.500
103. Irani RR, Callis CF. Metal complexing by phosphorus compounds. I. The thermodynamics of association of linear polyphosphates with calcium. *J Phys Chem*. 1960;64(10):1398–1407. doi:10.1021/j100839a010
104. Müller WEG, Neufurth M, Lieberwirth I, Wang SF, Schröder HC, Wang XH. Functional importance of coacervation to convert calcium polyphosphate nanoparticles into the physiologically active state. *Mater Today Bio*. 2022;16:100404. doi:10.1016/j.mtbio.2022.100404
105. Van Wazer JR, Campanella DA. Structure and properties of the condensed phosphates. IV. Complex ion formation in polyphosphate solutions. *J Am Chem Soc*. 1950;72(2):655–663. doi:10.1021/ja01158a004
106. Schepler H, Wang XH, Neufurth M, Wang SF, Schröder HC, Müller WEG. The therapeutic potential of inorganic polyphosphate: a versatile physiological polymer to control coronavirus disease (COVID-19). *Theranostics*. 2021;11(13):6193–6213. doi:10.7150/thno.59535
107. Müller WEG, Schepler H, Neufurth M, et al. The physiological polyphosphate as a healing biomaterial for chronic wounds: crucial roles of its antibacterial and unique metabolic energy supplying properties. *J Mater Sci Technol*. 2023;135:170–185. doi:10.1016/j.jmst.2022.07.018
108. Berube BJ, Bubeck Wardenburg J. *Staphylococcus aureus* α-toxin: nearly a century of intrigue. *Toxins*. 2013;5(6):1140–1166. doi:10.3390/toxins5061140
109. Baaske R, Richter M, Möller N, et al. ATP release from human airway epithelial cells exposed to *Staphylococcus aureus* alpha-toxin. *Toxins*. 2016;8(12):365. doi:10.3390/toxins8120365
110. Walev I, Martin E, Jonas D, et al. Staphylococcal alpha-toxin kills human keratinocytes by permeabilizing the plasma membrane for monovalent ions. *Infect Immun*. 1993;61(12):4972–4979. doi:10.1128/iai.61.12.4972-4979.1993
111. Clifton LA, Skoda MW, Le Brun AP, et al. Effect of divalent cation removal on the structure of gram-negative bacterial outer membrane models. *Langmuir*. 2015;31(1):404–412. doi:10.1021/la504407v
112. Müller WEG, Wang SF, Wiens M, et al. Uptake of polyphosphate microparticles *in vitro* (SaOS-2 and HUVEC cells) followed by an increase of the intracellular ATP pool size. *PLoS One*. 2017;12(12):e0188977. doi:10.1371/journal.pone.0188977
113. Wang X, Shi C, Mo J, Xu Y, Wei W, Zhao J. An inorganic biopolymer polyphosphate controls positively charged protein phase transitions. *Angew Chem Int Ed Engl*. 2020;59(7):2679–2683. doi:10.1002/anie.201913833
114. Docampo R, Jimenez V, Lander N, Li ZH, Niyogi S. New insights into roles of acidocalcisomes and contractile vacuole complex in osmoregulation in protists. *Int Rev Cell Mol Biol*. 2013;305:69–113. doi:10.1016/B978-0-12-407695-2.00002-0
115. Docampo R, Huang G. Acidocalcisomes of eukaryotes. *Curr Opin Cell Biol*. 2016;41:66–72. doi:10.1016/j.ceb.2016.04.007
116. Labberton L, Long AT, Gendler SJ, et al. A flow cytometry-based assay for procoagulant platelet polyphosphate. *Cytometry B Clin Cytom*. 2018;94(2):369–373. doi:10.1002/cyto.b.21492
117. Müller WEG, Neufurth M, Wang SF, et al. Amorphous, smart, and bioinspired polyphosphate nano/microparticles: a biomaterial for regeneration and repair of osteo-articular impairments *in-situ*. *Int J Mol Sci*. 2018;19(2):427. doi:10.3390/ijms19020427
118. Müller WEG, Schepler H, Tolba E, et al. A physiologically active interpenetrating collagen network that supports growth and migration of epidermal keratinocytes: zinc-polyP nanoparticles integrated into compressed collagen. *J Mater Chem B*. 2020;8(27):5892–5902. doi:10.1039/d0tb01240h
119. Neufurth M, Wang XH, Wang SF, Schröder HC, Müller WEG. Caged dexamethasone/quercetin nanoparticles, formed of the morphogenetic active inorganic polyphosphate, are strong inducers of *MUC5AC*. *Mar Drugs*. 2021;19(2):64. doi:10.3390/md19020064
120. Moore KA, Lemischka IR. Stem cells and their niches. *Science*. 2006;311(5769):1880–1885. doi:10.1126/science.1110542
121. Müller WEG, Tolba E, Schröder HC, et al. A new printable and durable *N, O*-carboxymethyl chitosan-Ca^{2+}-polyphosphate complex with morphogenetic activity. *J Mater Chem B*. 2015;3(8):1722–1730. doi:10.1039/c4tb01586j
122. Müller WEG, Neufurth M, Wang SF, Tolba E, Schröder HC, Wang XH. Morphogenetically active scaffold for osteochondral repair (polyphosphate/alginate/*N, O*-carboxymethyl chitosan). *Eur Cell Mater*. 2016;31:174–190. doi:10.22203/ecm.v031a12

123. Wang XH, Ackermann M, Tolba E, et al. Artificial cartilage bio-matrix formed of hyaluronic acid and Mg^{2+}-polyphosphate. *Eur Cell Mater*. 2016;32:271–283. doi:10.22203/eCM.v032a18
124. Tolba E, Wang XH, Ackermann M, et al. *In situ* polyphosphate nanoparticle formation in hybrid poly(vinyl alcohol)/karaya gum hydrogels: a porous scaffold inducing infiltration of mesenchymal stem cells. *Adv Sci*. 2018;6(2):1801452. doi:10.1002/advs.201801452
125. Neufurth M, Wang SF, Schröder HC, Al-Nawas B, Wang XH, Müller WEG. 3D bioprinting of tissue units with mesenchymal stem cells, retaining their proliferative and differentiating potential, in polyphosphate-containing bio-ink. *Biofabrication*. 2021;14:015016. doi:10.1088/1758-5090/ac3f29
126. Bjarnsholt T, Kirketerp-Møller K, Jensen PØ, et al. Why chronic wounds will not heal: a novel hypothesis. *Wound Repair Regen*. 2008;16(1):2–10. doi:10.1111/j.1524-475X.2007.00283.x
127. Müller WEG, Tolba E, Feng QL, et al. Amorphous Ca^{2+} polyphosphate nanoparticles regulate the ATP level in bone-like SaOS-2 cells. *J Cell Sci*. 2015;128(11):2202–2207. doi:10.1242/jcs.170605
128. Wang SF, Wang XH, Neufurth M, et al. Biomimetic alginate/gelatin cross-linked hydrogels supplemented with polyphosphate for wound healing applications. *Molecules*. 2020;25(21):5210. doi:10.3390/molecules25215210
129. Sarker B, Singh R, Zehnder T, et al. Macromolecular interactions in alginate−gelatin hydrogels regulate the behavior of human fibroblasts. *J Bioact Compat Polym*. 2017;32:309–324. doi:10.1177/0883911516668667
130. Schepler H, Neufurth M, Wang SF, et al. Acceleration of chronic wound healing by bio-inorganic polyphosphate: *in vitro* studies and first clinical applications. *Theranostics*. 2022;12(1):18–34. doi:10.7150/thno.67148
131. Müller WEG, Relkovic D, Ackermann M, et al. Enhancement of wound healing in normal and diabetic mice by topical application of amorphous polyphosphate. Superior effect of a host-guest composite material composed of collagen (host) and polyphosphate (guest). *Polymers*. 2017;9(7):300. doi:10.3390/polym9070300
132. McCarty SM, Percival SL, Clegg PD, Cochrane CA. The role of polyphosphates in the sequestration of matrix metalloproteinases. *Int Wound J*. 2015;12(1):89–99. doi:10.1111/iwj.12058
133. Müller WEG, Tolba E, Wang SF, et al. Nanoparticle-directed and ionically forced polyphosphate coacervation: a versatile and reversible core-shell system for drug delivery. *Sci Rep*. 2020;10(1):17147. doi:10.1038/s41598-020-73100-5
134. Wang XH, Schröder HC, Grebenjuk V, et al. The marine sponge-derived inorganic polymers, biosilica and polyphosphate, as morphogenetically active matrices/scaffolds for the differentiation of human multipotent stromal cells: potential application in 3D printing and distraction osteogenesis. *Mar Drugs*. 2014;12(2):1131–1147. doi:10.3390/md12021131
135. Hassanian SM, Ardeshirylajimi A, Dinarvand P, Rezaie AR. Inorganic polyphosphate promotes cyclin D1 synthesis through activation of mTOR/Wnt/β-catenin signaling in endothelial cells. *J Thromb Haemost*. 2016;14(11):2261–2273. doi:10.1111/jth.13477
136. Kawazoe Y, Katoh S, Onodera Y, Kohgo T, Shindoh M, Shiba T. Activation of the FGF signaling pathway and subsequent induction of mesenchymal stem cell differentiation by inorganic polyphosphate. *Int J Biol Sci*. 2008;4(1):37–47. doi:10.7150/ijbs.4.37
137. Shiba T, Nishimura D, Kawazoe Y, et al. Modulation of mitogenic activity of fibroblast growth factors by inorganic polyphosphate. *J Biol Chem*. 2003;278(29):26788–26792. doi:10.1074/jbc.M303468200
138. Wang XH, Schröder HC, Feng QL, Diehl-Seifert B, Grebenjuk VA, Müller WEG. Isoquercitrin and polyphosphate co-enhance mineralization of human osteoblast-like SaOS-2 cells *via* separate activation of two RUNX2 cofactors AFT6 and Ets1. *Biochem Pharmacol*. 2014;89(3):413–421. doi:10.1016/j.bcp.2014.03.020
139. Wang L, Fraley CD, Faridi J, Kornberg A, Roth RA. Inorganic polyphosphate stimulates mammalian TOR, a kinase involved in the proliferation of mammary cancer cells. *Proc Natl Acad Sci U S A*. 2003;100(20):11249–11254. doi:10.1073/pnas.1534805100
140. Müller WEG, Wang XH, Diehl-Seifert B, et al. Inorganic polymeric phosphate/polyphosphate as an inducer of alkaline phosphatase and a modulator of intracellular Ca^{2+} level in osteoblasts (SaOS-2 cells) *in vitro*. *Acta Biomater*. 2011;7(6):2661–2671. doi:10.1016/j.actbio.2011.03.007
141. Holmström KM, Marina N, Baev AY, Wood NW, Gourine AV, Abramov AY. Signalling properties of inorganic polyphosphate in the mammalian brain. *Nat Commun*. 2013;4:1362. doi:10.1038/ncomms2364
142. Suess PM, Tang Y, Gomer RH, Parent C. The putative G protein–coupled receptor GrlD mediates extracellular polyphosphate sensing in *Dictyostelium discoideum*. *Mol Biol Cell*. 2019;30(9):1118–1128. doi:10.1091/mbc.E18-10-0686
143. Müller WEG, Ackermann M, Tolba E, et al. Role of ATP during the initiation of microvascularization: acceleration of an autocrine sensing mechanism facilitating chemotaxis by inorganic polyphosphate. *Biochem J*. 2018;475(20):3255–3273. doi:10.1042/BCJ20180535
144. Liu H, Du Y, St-Pierre JP, et al. Bioenergetic-active materials enhance tissue regeneration by modulating cellular metabolic state. *Sci Adv*. 2020;6(13):eaay7608. doi:10.1126/sciadv.aay7608
145. Schwiebert EM, Zsembery A. Extracellular ATP as a signaling molecule for epithelial cells. *Biochim Biophys Acta*. 2003;1615(1−2):7–32. doi:10.1016/s0005-2736(03)00210-4
146. Tagliabracci VS, Wiley SE, Guo X, et al. A single kinase generates the majority of the secreted phosphoproteome. *Cell*. 2015;161(7):1619–1632. doi:10.1016/j.cell.2015.05.028
147. Wilson MR, Easterbrook-Smith SB. Clusterin is a secreted mammalian chaperone. *Trends Biochem Sci*. 2000;25(3):95–98. doi:10.1016/s0968-0004(99)01534-0
148. Wyatt AR, Yerbury JJ, Berghofer P, et al. Clusterin facilitates *in vivo* clearance of extracellular misfolded proteins. *Cell Mol Life Sci*. 2011;68(23):3919–3931. doi:10.1007/s00018-011-0684-8
149. Zhou L, Shi H, Li Z, He C. Recent advances in complex coacervation design from macromolecular assemblies and emerging applications. *Macromol Rapid Commun*. 2020;41(21):e2000149. doi:10.1002/marc.202000149
150. Aumiller WM Jr, Pir Cakmak F, Davis BW, Keating CD. RNA-based coacervates as a model for membraneless organelles: formation, properties, and interfacial liposome assembly. *Langmuir*. 2016;32(39):10042–10053. doi:10.1021/acs.langmuir.6b02499
151. Ono S, Imai R, Ida Y, Shibata D, Komiya T, Matsumura H. Increased wound pH as an indicator of local wound infection in second degree burns. *Burns*. 2015;41(4):820–824. doi:10.1016/j.burns.2014.10.023
152. Gwynne L, Williams GT, Yan KC, et al. TCF-ALP: a fluorescent probe for the selective detection of *Staphylococcus* bacteria and application in "smart" wound dressings. *Biomater Sci*. 2021;9(12):4433–4439. doi:10.1039/d0bm01918f

153. Alpaslan G, Nakajima T, Takano Y. Extracellular alkaline phosphatase activity as a possible marker for wound healing: a preliminary report. *J Oral Maxillofac Surg*. 1997;55(1):56−62;discussion 62–63−. doi:10.1016/S0278-2391(97)90447-X
154. Kogan S, Sood A, Garnick MS. Zinc and wound healing: a review of zinc physiology and clinical applications. *Wounds*. 2017;29(4):102–106. PMID: 28448263.
155. Ghahramani Z. Probabilistic machine learning and artificial intelligence. *Nature*. 2015;521(7553):452–459. doi:10.1038/nature14541
156. Nesbeth DN, Zaikin A, Saka Y, et al. Synthetic biology routes to bio-artificial intelligence. *Essays Biochem*. 2016;60(4):381–391. doi:10.1042/EBC20160014
157. Zhang YS, Khademhosseini A. Advances in engineering hydrogels. *Science*. 2017;356(6337):eaaf3627. doi:10.1126/science.aaf3627
158. Müller WEG, Neufurth M, Ackermann M, et al. Bifunctional dentifrice: amorphous polyphosphate a regeneratively active sealant with potent anti-*Streptococcus mutans* activity. *Dent Mater*. 2017;33(7):753–764. doi:10.1016/j.dental.2017.04.009
159. Schepler H, Wang XH, Neufurth M, Wang SF, Schröder HC, Müller WEG. The therapeutic potential of inorganic polyphosphate: a versatile physiological polymer to control coronavirus disease (COVID-19). *Theranostics*. 2021;11(13):6193–6213. doi:10.7150/thno.59535
160. Lorenz B, Leuck J, Köhl D, Muller WEG, Schröder HC. Anti-HIV-1 activity of inorganic polyphosphates. *J Acquir Immune Defic Syndr Hum Retrovirol*. 1997;14(2):110–118. doi:10.1097/00042560-199702010-00003
161. Neufurth M, Wang XH, Tolba E, et al. The inorganic polymer, polyphosphate, blocks binding of SARS-CoV-2 spike protein to ACE2 receptor at physiological concentrations. *Biochem Pharmacol*. 2020;182:114215. doi:10.1016/j.bcp.2020.114215
162. Ferrucci V, Kong DY, Asadzadeh F, et al. Long-chain polyphosphates impair SARS-CoV-2 infection and replication. *Sci Signal*. 2021;14(690):eabe5040. doi:10.1126/scisignal.abe5040
163. Müller WEG, Neufurth M, Lieberwirth I, et al. Triple-target stimuli-responsive anti-COVID-19 face mask with physiological virus-inactivating agents. *Biomater Sci*. 2021;9(18):6052–6063. doi:10.1039/d1bm00502b
164. Zhang L, He G, Yu Y, Zhang Y, Li X, Wang S. Design of biocompatible chitosan/polyaniline/laponite hydrogel with photothermal conversion capability. *Biomolecules*. 2022;12(8):1089. doi:10.3390/biom12081089
165. Barnese K, Gralla EB, Cabelli DE, Valentine JS. Manganous phosphate acts as a superoxide dismutase. *J Am Chem Soc*. 2008;130(14):4604–4606. doi:10.1021/ja710162n
166. Gray MJ, Jakob U. Oxidative stress protection by polyphosphate--new roles for an old player. *Curr Opin Microbiol*. 2015;24:1–6. doi:10.1016/j.mib.2014.12.004
167. Beaufay F, Quarles E, Franz A, Katamanin O, Wholey WY, Jakob U. Polyphosphate functions *in vivo* as an iron chelator and Fenton reaction inhibitor. *mBio*. 2020;11(4):e01017–e01020. doi:10.1128/mBio.01017-20
168. Xie M, Liu X, Wang S. Degradation of methylene blue through Fenton-like reaction catalyzed by MoS_2-doped sodium alginate/Fe hydrogel. *Colloids Surf B Biointerfaces*. 2022;214:112443. doi:10.1016/j.colsurfb.2022.112443
169. Guitart-Mampel M, Urquiza P, Carnevale Neto F, et al. Mitochondrial inorganic polyphosphate (polyP) is a potent regulator of mammalian bioenergetics in SH-SY5Y cells: a proteomics and metabolomics study. *Front Cell Dev Biol*. 2022;10:833127. doi:10.3389/fcell.2022.833127
170. Solesio ME, Xie L, McIntyre B, et al. Depletion of mitochondrial inorganic polyphosphate (polyP) in mammalian cells causes metabolic shift from oxidative phosphorylation to glycolysis. *Biochem J*. 2021;478(8):1631–1646. doi:10.1042/BCJ20200975
171. Hambardikar V, Guitart-Mampel M, Scoma ER, et al. Enzymatic depletion of mitochondrial inorganic polyphosphate (polyP) increases the generation of reactive oxygen species (ROS) and the activity of the pentose phosphate pathway (PPP) in mammalian cells. *Antioxidants*. 2022;11(4):685. doi:10.3390/antiox11040685